AN INTEGRATED FRAMEWORK AND SOFTWARE PROTOTYPE FOR MULTISCALE ENERGY SYSTEMS ENGINEERING

A Thesis

by

RAHUL KAKODKAR

Submitted to the Office of Graduate and Professional Studies of
Texas A&M University
in partial fulfillment of the requirements for the degree of

MASTER OF SCIENCE

Chair of Committee,	Efstratios N. Pistikopoulos
Committee Members,	Mahmoud El-Halwagi
	Le Xie
	M. M. Faruque Hasan
Head of Department,	Arul Jayaraman

August 2021

Major Subject: Chemical Engineering

ABSTRACT

In this work, the developments of ENERGIA, a multi-scale energy systems transition modeling, optimization and scenario analysis framework and software prototype are presented. ENERGIA integrates (i) energy supply chain and transportation considerations, (ii) detailed energy production aspects, and (iii) scheduling decisions for operation and inventory management of energy and resources storage. It is based on a methodology that involves (i) detailed data and models for the description of process alternatives and units and the corresponding supply chains, (ii) a library of surrogate modeling techniques, for both the nonlinear process models, as well as scheduling decisions, and (iii) a detailed design planning time-varying scheduling model (iv) a mixed-integer programming optimization strategy. ENERGIA's python-based environment allows users to visualize resource availability and demands at various temporal and geographic scales and resolutions, and compare competing objectives and renewable-based energy strategies. A hydrogen-economy energy transition problem is presented to highlight the key capabilities of the proposed framework.

DEDICATION

To my mother Anjali, her mother Kumudhini, and our collective mother, nature. All of whom continue to nurture and guide me.

ACKNOWLEDGMENTS

I would like to thank my advisor Prof. Efstratios N. Pistikopoulos whose mentorship and pursuit of research excellence continues to inspire me. This work would not have been possible without the support of my colleagues in the Multi-parametric Optimization & Control (MPOC) Group, as also the faculty and my colleagues in the Texas A & M Energy Institute and the Artie McFerrin Department of Chemical Engineering.

CONTRIBUTORS AND FUNDING SOURCES

Contributors

This work was supported by a thesis committee consisting of Professors Efstratios N. Pistikopoulos, Mahmoud El-Halwagi, Le Xie, and M. M. Faruque Hasan. ENERGIA was originally conceptualized by Prof. Efstratios N. Pistikopoulos. The data utilized in the study was collected from earlier works from the MPOC group, chiefly from the works of Drs Doga Demirhan, William Tso and Styliani Avraamidou. R. Cory Allen, Stefanos Baratsas, and Marcello Di Martino are also part of the team working on ENERGIA. Lastly, Drs Clara F. Heuberger, Mark Klokkenburg, and Joseph B Powell from Shell Global Solutions International B.V. have overseen the development of ENERGIA.

The work presented in Appendix A was co-authored with a team of researchers from MIT Energy Initiative. Namely, Drs Gunnan He, Maryam Arbabzadeh, Dharik Mallapragada, Ian Miller, and Emre Gençer.

All other work conducted for the thesis was completed by me independently.

Funding Sources

My graduate research is funded by the Artie McFerrin Deparment of Chemical Engineering, the Texas A&M Energy Institute, and Shell Global Solutions International B.V.

NOMENCLATURE

AC	Alternating Current
AHC	Agglomerative Hierarchical Clustering
AM	Amarillo, Texas
Btu	British thermal unit
CAES	Compressed Air Energy Storage
CEC	California Energy Commission
CGE	Computable General Equilibrium
CO_2^e	Carbon Dioxide Emitted
DC	Direct Current
DEC	Dense Energy Carrier
DHI	Direct Horizontal Irradiance
DNI	Direct Normal Irradiance
DOE	Department of Energy
EFOM	Energy Flow Optimization Model
ERCOT	Electric Reliability Council of Texas
EV	Electric Vehicle
GAMS	Generalized Algebraic Modeling System
GDP	Gross Domestic Product
GHI	Global Horizontal Irradiance
GHG	Greenhouse Gases
GTL	Gas to Liquid
GWP	Global Warming Potential

INDC	Intended Nationally Determined Contribution
LCA	Lifecycle Assessment
LP	Linear Program
MARKAL	MARket ALlocation
MED	MARKAL elastic demand model
MH	Metal Hydride
MIP	Mixed Integer Program
MILP	Mixed Integer Linear Program
MINLP	Mixed Integer Non-linear Program
NaS	Sodium Sulfur
NLP	Non-linear Program
NREL	National Renewable Energy Laboratory
NSRDB	National Solar Radiation Database
PSH	Pumped Storage Hydropower
RS	Riverside, California
RTN	Resource Task Network
SDG	Sustainable Development Goals
TIMES	The Integrated MARKAL-EFOMSystem
VRE	Variable Renewable Energy

TABLE OF CONTENTS

LIST OF FIGURES

LIST OF TABLES

TABLE Page

1. INTRODUCTION

The de-carbonization of our energy infrastructure, while meeting a growing global energy demand, requires a shift in primary energy production and supply towards renewable technologies. Renewables, such as wind, solar and biofuels, are typically available intermittently, and are subject to seasonal variability, uneven geographic access and distribution. This necessitates the explicit consideration of spatiotemporal characteristics and variabilities in the analysis of proposed low-carbon transition and future energy scenarios. Future energy systems will likely involve a greater degree of integration amongst its value chains across multiple energy sectors with competing technology options for sustainable energy generation, production of chemicals energy carriers and synthetic fuels, and multiple modes for both freight and public transportation [1]. A holistic, multiscale energy systems engineering approach can be used to develop a systematic framework to assess promising energy transition pathways by linking decisions at the process synthesis, scheduling and supply chain level, and enabling trade-off analyses.

To this end, various data-driven energy system modeling, forecasting, and optimization frameworks have been developed in the recent years [2, 3, 4]. Applications include multi-period nonlinear production planning [5], optimal natural gas utilization [6], renewable power generation and storage optimization [7], and sustainable chemicals production [8], amongst other things. Given that the ongoing penetration of renewable energy into the energy market has been dominated by variable renewable energy (VRE) sources such as solar and wind, with a 91% share in the renewable energy generation capacity added in 2020 [9], most proposed models feature VRE sources prominently. Nonetheless, it is clear that energy systems should involve a comprehensive set of technology, resource, and transportation options. The representation of such extensive networks under a unified framework is naturally challenging.

ENERGIA, at its core, relies on resource task network (RTN) representation and mixed integer linear programming (MILP) techniques to mathematically model and optimize multi-scale energy systems. This approach combines and takes advantage of the synergistic elements in process syn-

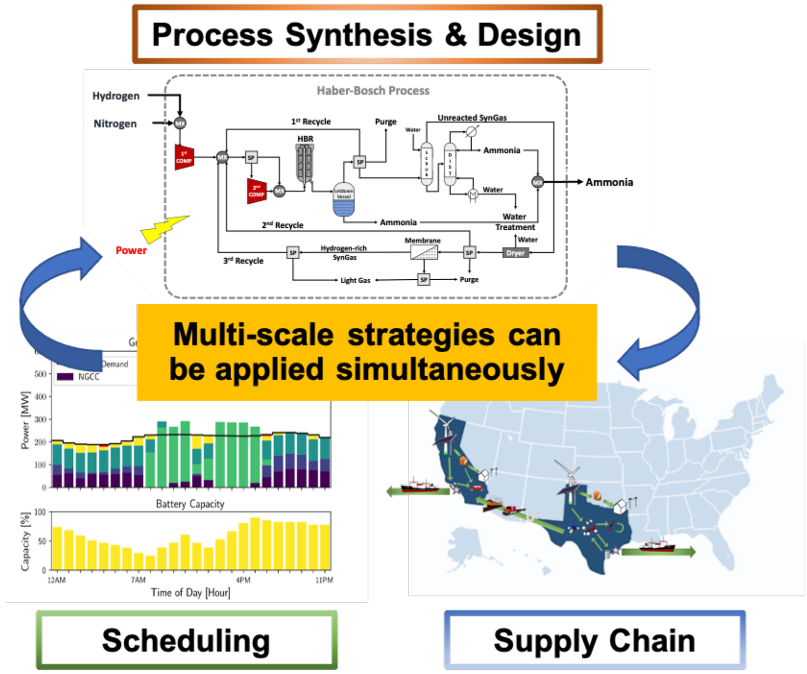

Figure 1.1: Integrated design, scheduling, and supply chain model

thesis and design, scheduling, and supply chain decisions while allowing for unification as shown in fig 1.1. A library of high-fidelity gPROMS models lends rigor to the formulations and provides accurate process modeling and cost parameters. Surrogate model approximation functions can be used along with embedded heuristics [10] to linearize process models to tame model complexity while also ensuring that an optimal solution is attained in feasible time. The high-fidelity models can then be used to validate the solution to ascertain accuracy and feasibility. Furthermore, visualization functions allow for an in-depth view and understanding of variability across various geographic and temporal scales.

For a more detailed explanation of the state-of-the-art in multiscale systems analyses and optimization, the reader can refer to the recently submitted paper [1] in appendix A. The rest of thesis is arranged as follows: in chapter 2 the motivation for the energy transition and the need for and utility of a unified framework and modeling tool is presented; in chapter 3 elements of a future hydrogen network formulation are represented and the key features of ENERGIA are highlighted; chapter 4 is dedicated to the summary and future work to be undertaken.

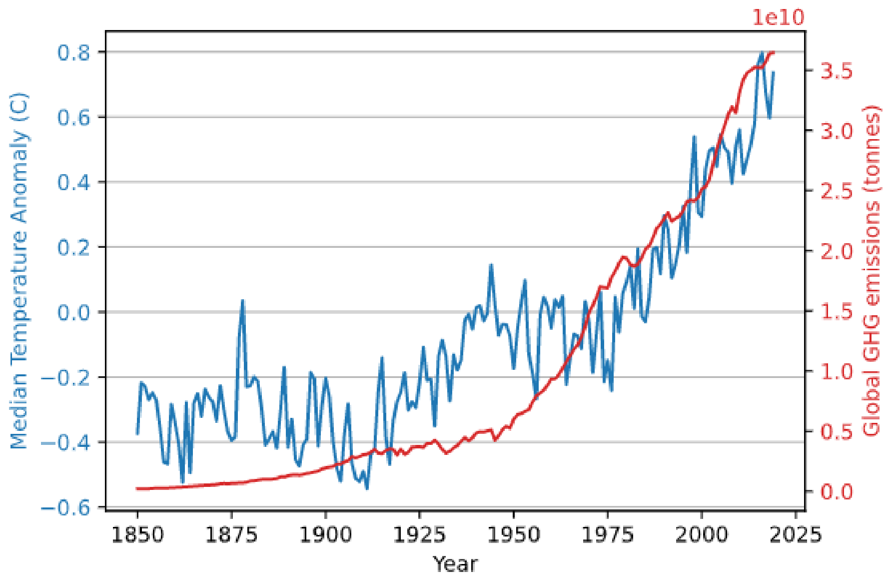

Figure 2.1: Global rise in temperature and GHG emissions

Greenhouse gas (GHG) emissions have been largely held responsible for the global rise in temperatures. To sustain quality of life and economic progress, several researchers [11, 12] and agencies [13, 14] have set a target of restricting the global rise (see fig. 2.1) in temperature to under $1.5 - 2^0$C as compared to pre-industrial levels by the year 2050. It is also imperative to recognize the distributed nature of emission (see fig. 2.2) as also the unifying nature of energy generation as a key contributor to emissions, and the transition towards more sustainable technology and configurations as a quantifiable analytical goal.

Moreover, storage and conversion technologies serve as synergistic elements that allow the transmutation of material resources to energy, and vice versa. Given the context, methodologies that consider the various sub-systems in a energy system under an integrated framework, allow decision makers to evaluate the trade-offs between different resource, technology, and transportation

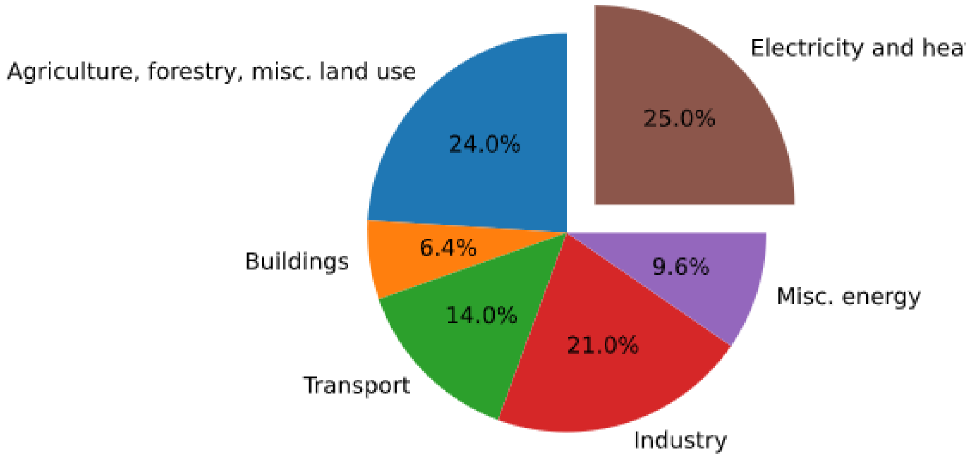

Figure 2.2: Sector-wise contribution to global GHG emissions

options. While also providing operational and scheduling decisions that are cognizant of resource availability and variability, technical limitations, system boundaries, uncertainty, as also localized policy restrictions and demographic factors.

To this end, energy systems modeling tools are critical towards conceptualizing and evaluating various technological and policy driven energy transition scenarios. To allow for integrated assessment of multiscale energy systems, tools should be able to compute energy balances inclusively at all levels of an energy system. This warrants the comprehensive inclusion of primary energy resources, conversion and storage technologies, supply chain and transportation networks, as well as demand characteristics and the effects of policy initiatives.

Amongst the earliest such vertically integrated models were MARKAL (a concatenation of MARKet ALlocation) [15] and Energy Flow Optimization Model (EFOM) [16, 17]. MARKAL , a Generalized Algebraic Modeling System (GAMS) [18, 19] language based multi-location mathematical modeling tool, provided a technology-rich basis for estimating energy dynamics over a multi-period horizon. MARKAL modeled systems as a linear programming which could simultaneously provide investment, operating, and supply decisions. Nonetheless, MARKAL was optimized to the objective of minimizing global costs.

Subsequently, the MARKAL elastic demand model (MED) model was developed over the MARKAL model to allow the analyses of low carbon scenarios in the Untied Kingdom (UK) [20]. It included updated fossil resource costs, expanded categorisation of carbon capture, wind resources and biomass chains to all end-use sectors, new hydrogen (H_2) infrastructures, and an improved treatment of electricity intermittency. Most notably, it introduced a range of constraints to represent policy changes, taxes, and subsidies. Nonetheless, neither MARKAL nor MED allowed spatial or temporal disaggregation, making even daily decisions such as location-specific supply-demand balancing elusive.

EFOM, again a bottom-up energy model, provided a detailed insight into energy flows at the technological levels for various European energy markets. Later, it was also specified in GAMS [21]. The two models were subsequently combined to form The Integrated MARKAL-EFOM System (TIMES) [22]. TIMES provides some additional features, not present in earlier models, such as variable time periods, detailed cash flow representation in the objective, flexible input and output for technologies, an integrated climate module, risk analyses, and endogenous energy trade between regions. TIMES again uses GAMS to generate either a linear program (LP) or a mixed integer program (MIP) which can be solved using commercially available solvers such as CPLEX [23].

Coarse time-steps, characteristic to computable general equilibrium (CGE) or partial equilibrium models, can often lead to an under-representation of temporal variability which is exacerbated with the large scale penetration of VREs [24]. This can in turn lead to an overestimation of the availability of renewable resources and an underestimation of the necessary investment [25]. Given the increasing share of renewables and electrification as a result of the ongoing energy transition, modeling and optimization tools that seek to resolve future energy systems need to consider both a finer temporal resolution and a longer time horizon.

To this end, many models have been developed that allow for long term planning with a fine temporal resolution but they are largely sector-specific such as electricity planning, power storage, heat integration, vehicular emissions [26, 27, 28, 29]. As such, most only resolve a particular aspect of the problem, such as GHG emissions [2] or cost. While these indeed serve as powerful tools for the analyses of energy systems at various scales, and can be used in conjunction to provide a detailed view of an energy transition scenario, there is still a need for a unified platform that allows for multiscale energy system engineering analyses. Furthermore, no currently available software paradigm allows for the integration of chemicals production, temporal variability on both the supply as well as the demand side, capacity based costing and process parameters, validation using high fidelity simulation models, while still adhering to a multi-location, multi-period formulation.

Figure 2.3: Design of supply chain between Texas and California

To elucidate upon the attributes of such an integrated framework, we present a model that seeks to utilize the renewable energy potential of Texas and California to meet the transportation energy requirements of California. This includes utilizing the solar and wind potential of both locations, in tandem, to produce dense energy carriers (DECs) such as hydrogen, ammonia, and methanol, as also the production of biofuels using biomass, and natural gas technologies. The multi-scale, multi-facility and multi-product paradigm should include time-dependent performance coefficients for technologies, as also time variant and location-dependant cost parameters associated with the constituent processes, and the effects of cost learning. [30].

Moreover, specific resource limitation with respect to the construction and start-up of candidate facilities need to be identified. Another stated goal is the inclusion of time-dependant carbon credits with the goal of delivering emission-free hydrogen and gas to liquid (GTL) fuels. The calculation of emissions need be comprehensive and over the lifetime of use of the proposed technologies. Furthermore, given the implementation of the software prototype to evaluate multi-location models and for transportation applications, existing and potential sites for infrastructure such as pipelines, hydrogen and electricity fueling stations have to be evaluated. Solution strategies to consider the time-lag in production and delivery will also need to be identified. There is also a need for methodologies that allow for comprehensive validation, uncertainty and flexibility analyses.

To generate and evaluate the trade-off between energy transition scenarios and technology pathways, we need accurate forecasting of the future demand for hydrogen and GTL fuels, as well as weather data that impacts solar and wind energy generation potential. The framework can subsequently be expanded to evaluate the possibility of meeting the energy demands of geographically distant locations through the ports of Los Angeles and Long Beach.
The framework and software prototype consider the following as inputs:

1. Time and location dependent resource availability
2. Time and location dependent energy demand
3. Model surrogates and linearized input-output parameter models of energy conversion technologies
4. Location specific and time-varying capital investment costs
5. Metrics such as global warming potential (GWP) and ozone-depletion potential to ascertain the life-cycle impact of technology.

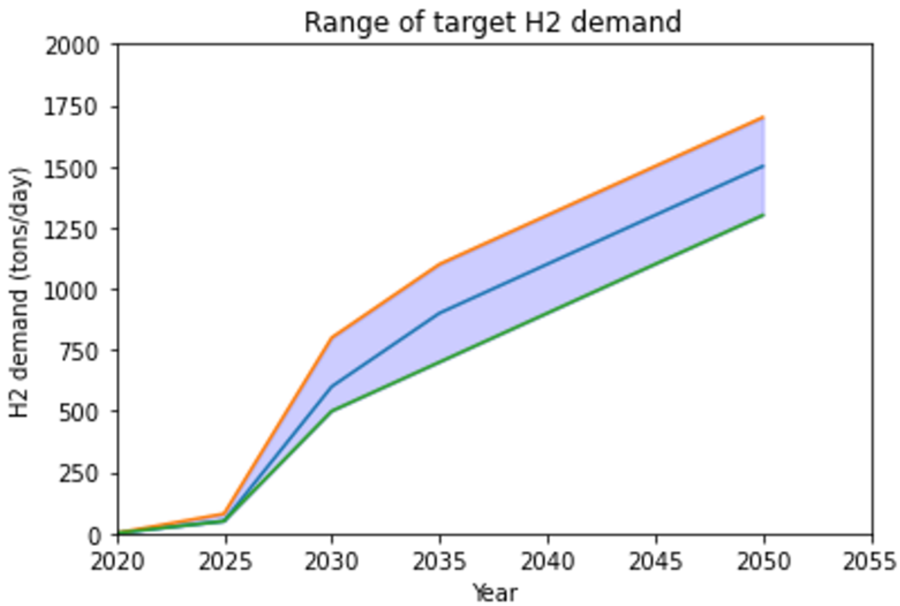

Figure 2.4: Future demand for hydrogen

6. Access to available transportation and storage infrastructure, as well as candidate locations for potential development.

And return an optimal solution that comprises:

1. Process and storage unit capacities
2. Time dependent production rates for each process
3. Material and energy flow rates between processes
4. Unit commitment and operating mode selections for processes
5. Inventory management decisions for storage of material and energy.
6. Transportation networks to describe the flow of material and energy.

The full mathematical model formulated for the system is described in the appendix B.

As a base case we evaluate the viability of producing hydrogen in two locations, namely Amarillo, Texas (AM) and Riverside, California (RS). Amarillo was chosen because of its proximity to existing oil and gas infrastructure, low land cost, and the availability of industrial water which will be required for the production of green hydrogen using electrolysis. Whereas, Riverside was chosen given its proximity to Los Angeles and the ports of Los Angeles and Long Beach. Moreover, RS has seen the establishment of three solar projects in the last decade by NextEra Energy Inc., with a total added capacity of 735 MW [31]. It is imperative to note that although water is available in Riverside as well, California's water resources have been under pressure in the recent years. Historically, the San Bernardino valley has been the preferred location for solar projects in California, and can also serve as a candidate location. Nonetheless, the viability of utilizing California's ample solar and wind potentials, as also the impact of green hydrogen production on the strained water resources mandate a careful study. In the subsequent subsections we provide a brief overview of the energy economies of California (subsection 2.1) and Texas (subsection 2.2) , and the role of hydrogen as an energy vector (subsection 2.3).

2.1 California - An energy perspective

California, the largest and most populous economy in the US has amongst the lowest energy consumption on a per capita basis in the US at 202 MMBTU, compared to 498 MMBTU in Texas, with the highest being 967 MMBTU in Wyoming, and[32]. This disproportionality can be largely explained by the different levels of urbanization in the states. As per the 2010 US Census [33], California with over a 95% urban population was the most urbanized state in the country, higher than Texas (84.7%) and Wyoming (64.8%). The agglomeration of population driven by urbanization, in itself, serves as a key driver towards reducing per capita energy consumption as well as the investment towards energy infrastructure.

In terms of policy, California has been particularly aggressive in establishing decarbonization targets [34, 35, 36, 37]. In particular, Assembly Bill 32 (AB 32) set the target of reducing emissions to 1990 levels by 2020, and Senate Bill 32 (SB 32) which aims to reduce emissions to at least 40 percent below 1990 levels by 2030. The earliest amongst the many environmentally conscious policies, Assembly Bill 1493 [38], aimed to reduce vehicular GHG emissions. Further, the bill recognized the threat of global warming to the state which is infact the fifth largest economy on the planet. Identified risks include prolonged water shortages due to changes in the snow-cap levels in the Sierra Nevada mountains, and purported health related effects due to air pollution. This was followed by specific bills aimed at designing transportation networks in conjunction with establishing sustainable communities [39], improving California's recycling capabilities [40], and protecting vulnerable communities [41].

In the last two decades, the in-state energy generating capacity across all sources has varied between a low of 186,815 GWh in 2002 and a high of 218,604 GWh in 2006. The value stood at 200,475 GWh in 2019. Nonetheless, this belies the underlying large-scale transition towards alternative energy sources. As per CEC data [42], coal saw a reduction of over 90% in the same time frame. This was replaced by VREs, with wind energy growing by 322% and solar now producing over 26,000 GWh compared to a mere 3 GWh in 2001. However, despite the tremendous potential for biomass in California, the sector remains underutilized with a contribution between 5500 - 7000 GWh in the last few decades. The large scale adoption of renewable technologies has helped curtail GHG emissions, which peaked at 490.9 $MMTCO_2^e$ in 2003, to 425.3 $MMTCO_2^e$ in 2018 despite the 17% increase in population and 59% increase in GDP. This amounts to a 22% and 43% reduction in emission per capita and per GDP unit respectively. The ongoing transition is best illustrated in the reduced GHG contribution by the electric power sector which reduced from 121.9 $MMTCO_2^e$ in 2001 to 63.1 $MMTCO_2^e$ in 2018. On the other hand, the transportation sector is still the dominant contributor, accounting for over 41% of total GHG emissions.

It is important to note that California is also a major importer of energy, in fact imported electricity contributed to a larger amount of GHG emissions than in-state produced electricity. While both have witnessed substantial reductions, in-state and imported energy still differ in carbon-intensity, 0.32 in 2001 to 0.18 tonne CO_2^e per MWh in 2018 in the case of the former, and 0.68 to 0.25 tonne CO_2^e per MWh for the latter in the same time frame [42]. To achieve decarbonization targets, California will need to import energy that is produced and transported sustainably. Texas, especially the panhandle region which receives high solar irradiance and wind speeds for a better part of the year, is an ideal candidate to meet California's energy demand. Moreover, the presence of major ports such as the Port of Los Angeles and the adjoining, but independent, Port of Long Beach in California raises the prospect of exporting energy to meet the demands of distant regions through marine transport.

2.2 Texas - An energy perspective

Texas, with the second largest population, has the second largest economy in the US, both behind California. Both states enjoy a high degree of urbanization and a diversified economies with ample representation from the manufacturing and the service sectors. However, Texas is both the largest energy producing and consuming state in the US. The state also enjoys a high level of solar irradiance and wind speeds year round, especially in the panhandle region. Furthermore, the presence of established oil and gas industry in the state, provides the prospect of utilizing existing infrastructure and human capital to drive the transition by producing bio-fuels and dense energy carriers (DECs) through renewable and sustainable means.

Texas is also the top crude oil and natural gas producing state. Through its 31 petroleum refineries, Texas processes about 5.3 million barrels of crude oil which is 43% of the nation's total production [43]. In fact, 26% of the total natural gas marketed in the US comes from the state. However, energy production in Texas is not limited to fossil fuels as it also leads the nation in the production of wind energy, amounting to 28% the total wind energy produced in the US[43]. Notably, natural gas is replacing coal as an energy feedstock. In the last decade, Texas surpassed the high production of natural gas seen in the 70s to now stand over 9,200 Trillion MMBtu in 2020 [44]. Meanwhile, the already plummeting share of coal generated energy is set to decrease further by 13% by 2030 to 73 billion kWh [45]. In 2020, Texas was the country's second-largest producer, after California, of solar photovoltaic (PV)-sourced power. Texas added 2.5 GW to its solar capacity in 2020 to almost double the total, this is expected to grow to 14.9 GW by 2022 [46].

On the legislative side, Texas recently passed a comprehensive emission reduction bill [47], and signed senate bills 2 and 3 into law to reform the Electric Reliability Council of Texas (ERCOT), and weatherize and improve the reliability of the state's power grid [48]. Moreover, Energy and Water Research Integration Act of 2019, was sponsored by a Texan legislator and requires the Department of Energy (DOE) to integrate water considerations into its energy research, development, and demonstration programs and projects [49].

2.3 Hydrogen, and hydrogen-based energy carriers

The utility of dense energy carriers (DECs) is manifold and along with other non-chemical storage options they can greatly reduce storage losses and the demand for virgin material needed for the manufacture of batteries. Besides, they are also ideal for long term storage, transportation, and are not geographically limited as in the case of pumped storage hydropower (PSH) and compressed air energy storage (CAES). However, for their use to generate power, investment towards back to power conversion technology such as turbines and fuel cells is necessary.

Hydrogen has drawn much attention as a DEC to work as a proxy for the temporally and geographically asynchronous deployment of energy. Noticeably, hydrogen is a dense form of energy (33.3 kWh/kg) but is limited by low volumetric capacity (2.5 kWh/L as a liquid). Factors such as the need to establish new infrastructure, safety concerns, and a bottleneck in terms of supplying sustainably produced (green) hydrogen have however restricted the penetration of hydrogen as an energy source. A key challenge is storage, hydrogen can be stored either cryogenically as a liquid at 20.35 K or as a compressed gas which requires a pressure of 350-700 bar. Metal hydride (MH) storage systems are also being investigated as a potential technology to store and deliver hydrogen [50].

Thus, ammonia and methanol have both been considered as DECs given their relatively higher volumetric energy densities of approximately 4.3 kWh/L and 4.6 kWh/L. These can both be produced from hydrogen in established industries and deployed through supply chains that take advantage of existing infrastructure. Moreover, ammonia can be stored as a liquid under moderate pressures of 10 - 20 bar or cryogenically at 239.85 K. Methanol is a liquid at room temperature. Nonetheless, currently the production of methanol is from carbon sources and the energy supply required for the production process can result in carbon emissions. Naturally, there are additional costs attached to their production. Nevertheless, the production of chemicals for energy storage is still attractive as these process can be scaled up with comparative ease. Moreover, DECs can be

Storage Attribute	CAES	Battery	PSH	H2 (L)	H2 (G)	NH3	CH3OH
H2 by weight (%)	-	-	-	100	100	17.8	12.6
Density (kg/m3)	-	-	-	71.2	24-40	105	99.8
Energy Density - (kWh/kg) Gravimetric	0.05	0.3	0.001	33.3	33.3	5.1	6.4
Energy Density - (kWh/L) Volumetric	0.001	0.7	0.001	2.5	1.0	4.3	4.6
Temperature (°C)	20	-20 to 60	20	-253	20	-33.3/20	20
Pressure (atm)	300	1	1	1	350-700	1/10-20	1
Duration	Hrs	Days	Mths	Mths	Mths	Mths	Mths

Table 2.1: A comparison of storage options and technologies

used to meet the demands of geographically distant regions as the storage losses are minimal. As a proof of concept, the CO_2-free Hydrogen Energy Supply-chain Technology Research Association (HySTRA) debuted the ship *Suiso Frontier* which saw hydrogen shipped 5,600 miles from south-east Australia to the Japanese city of Kobe[51]. A comparison of the various attributes of different storage technologies is provided in table 2.3.

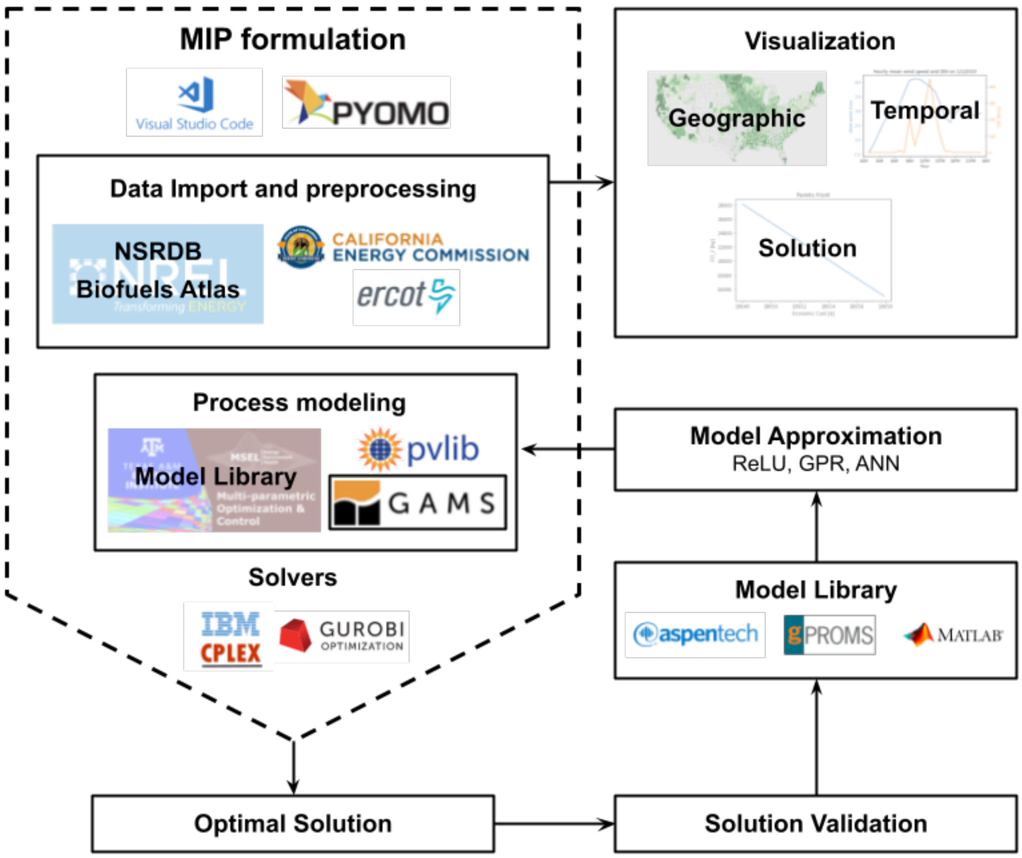

Figure 3.1: Constituent modules in ENERGIA

In the following section we illustrate the solution methodology to resolve the simultaneous design and operation of a hydrogen supply chain using the features in ENERGIA. In the example, we seek to evaluate the viability of producing hydrogen using alkaline water electrolysis.

We allow multiple energy storage options, viz. PSH, CAES, NaS batteries. Further, both solar and wind can be used to the meet the power demand. Although, the model allows purchase from the grid, none of the cases studied utilized this option. Additionally, given the mobility demand can also be met using electricity, we provide the option of generating AC power using a DC to AC inverter. Power can be produced using a hydrogen fuel cell as well.

Hydrogen can be stored in two forms, either as liquefied cryogenic hydrogen or as pressurized hydrogen.

3.1 Data acquisition and representation

Data-driven optimization techniques rely on accurate data, available at appropriate temporal and geographic resolutions. Several databases, often free, can be accessed to obtain data on temporal and geographic availability of resources as well as the demand for energy and products such as transportation fuels and chemicals. Prominently, National Renewable Energy Laboratory (NREL) hosts databases such as the National Solar Radiation Database (NSRDB) which provides data for solar irradiance and wind speeds at five minute intervals, the Renewable Energy (RE) Atlas which provides the energy potential of various renewable energy resources, the Biofuels Atlas which gives a breakdown of the different biomass derived energy feedstocks available. All the aforementioned data sets are at least available at a county level geographic resolution. Further, local energy commissions can be accessed for electricity demand and prices, such as the California Energy Commission (CEC) or the ERCOT.

The availability of solar energy, for example, can be estimated using meteorological data such as location-specific direct normal irradiance (DNI). Similarly, wind energy availability can be calculated using wind speed data. Given the option of grid electricity purchase, the temporal data for cost of electricity purchase from the grid can also be obtained. Further, aggregated location-specific energy demand, bio-energy availability, land costs, energy demand for transport can be accessed.

Providing time variant data increases the analytical scope of the model and provides more accurate outputs that implicitly account for temporal characteristics and variability. Solutions for storage requirements to address the problems of intermittency, production targets that match the demand, and supply chain and transportation decisions can be obtained simultaneously. Optimized to a cost objective, the solution can meet the demand at the lowest capital investment, while reduc-

dhi	dni	ghi	wind_speed	T$_air$	T$_dew$	humidity	Solar	Wind	ERCOT_w

Table 3.1: Sample header for generated dataframe

ing the requirement for storage and avoiding over-production.

In the subsequent sub-sections, the embedded functions in ENERGIA for handling data are highlighted. The data is categorized under temporal data in 3.1.1 and geographic data 3.1.2.

3.1.1 Temporal data

ENERGIA's *energia.data_import()* function has the ability to import available data in the native comma separated values (*.csv*) format. However, the functionality is not limited to acquiring data as the function also implicitly calculates the solar and wind power generation potentials to form a comprehensive data structure of the *pandas.DataFrame()* class. The sample header of the dataframe for AM is shown in table 3.1.1. The function utilizes the direct horizontal irradiance (DHI), direct normal irradiance (DNI), global horizontal irradiance (GHI), ambient air temperature, dew point, relative humidity data and feeds it to the pvlib python [52] module developed by NREL to calculate the solar power generation potential. Similarly, wind speed is used to calculate wind power generation potential using an empirical equation. Solar and wind data is available at a 5 minute interval starting from the year 2018, and at hourly intervals prior to that. However, the electricity demand data as shown in the last column for the appropriate ERCOT region is only available at an hourly interval. Thus, the hourly means are used to produce a uniform data structure with 8760 data points with each data point representing an hour in a calendar year.

Further, specific resources can also be accessed, such as solar power generation data using the *energia.only_solar_output()* function and the wind power generation data using the *energia.only_wind_output()* function. Moreover, if the user wishes to view solely the potential for renewable power generation, the *energia.only_renewables()* function can be used. The function trims the dataframe to provide only the solar and wind power potential.

3.1.2 Geographic data

The *energia.AMERICA()* function allows the user to access the biomass and biofuels availability of every county in the US again as a *pandas.DataFrame()*. This includes the availability of bagasse, sorghum, barley, mill refuse, lumber residue, rice straw, wheat straw, and corn stover.

The *energia.biomass_profile()* function allows the user to view a breakdown of the biomass availability of a county at a glance. Note that here, the values are again drawn from the dataframe created by the *energia.AMERICA()* function. The sample output for the biomass profile of Potter county (Amarillo being the county seat) is presented in fig. 3.2.

```
gid
2709    0.0
Name: bagasse, dtype: float64gid
2709    0.0
Name: barley_straw, dtype: float64gid
2709    0.0
Name: corn_stover, dtype: float64gid
2709    273.7
Name: grain_sorghum_stubble, dtype: float64gid
2709    0.0
Name: rice_straw, dtype: float64gid
2709    1148.0
Name: wheat_straw, dtype: float64total: gid
2709    1421.7
dtype: float64
```

Figure 3.2: sample output of the *biomass_profile()* function for Potter county

If the user needs to access any particular value, the *energia.get_geo_info()* function can be used. This allows the user to access data such as the area (fig. 3.3) of the county as well as methane emissions from specific sources such as industrial (fig. 3.4), waste water, landfill, and manure.

3.2 Visualization libraries

Energy systems analyses requires insights into how the systems function at various temporal and geographic scales. This is especially relevant for the inclusion of renewable energy such as solar and wind which are subject to daily, seasonal, as well as geographic variations. ENERGIA

```
gid
217    849.2363
Name: area, dtype: float64
```

Figure 3.3: sample output of the *get_geo_info()* function for area of Riverside county

```
gid
217    86.0254
Name: industrial_methane, dtype: float64
```

Figure 3.4: sample output of the *get_geo_info()* function for industrial methane emissions of Riverside county

allows users to plot data at user defined temporal and geographic resolutions.

3.2.1 Time series plots

The *energia.ts_plot()* function for example provides a time series plot at user-defined temporal resolutions as shown in figs 3.5 and 3.6. Further, time series plots can be plotted for any attribute available in the dataframe generated by the *energia.data_import()* function.

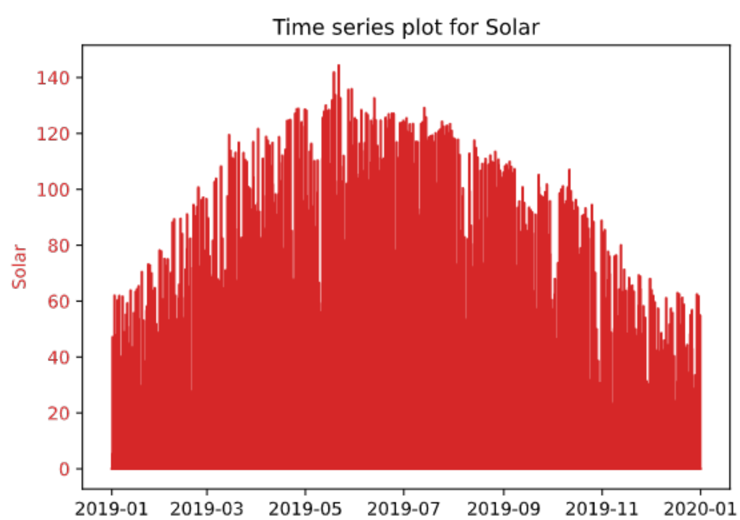

Figure 3.5: Time series plot of daily average solar potential in Watts for Amarillo, Texas

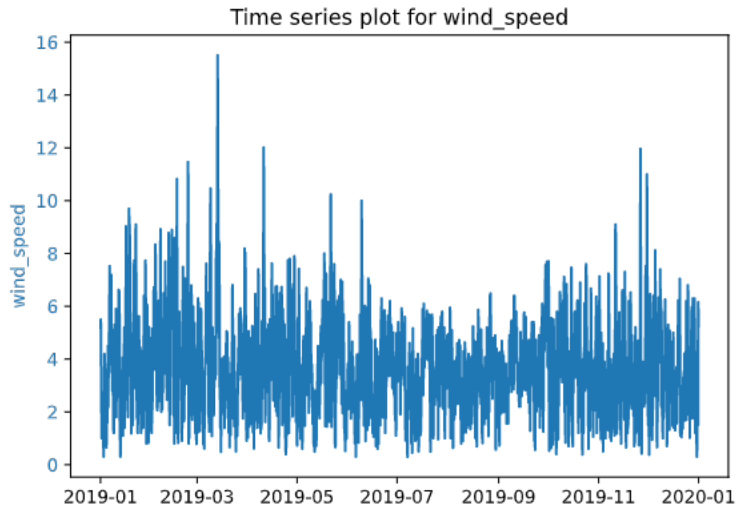

Figure 3.6: Time series plot of wind speed in m/s in Amarillo, Texas

Moreover, the user might also be interested in looking at the interplay of solar and wind to understand the potential for sector coupling. For this purpose, ENERGIA also provides specific plotting functions such as *energia.plot_day_dni_wind()* as shown in fig 3.7.

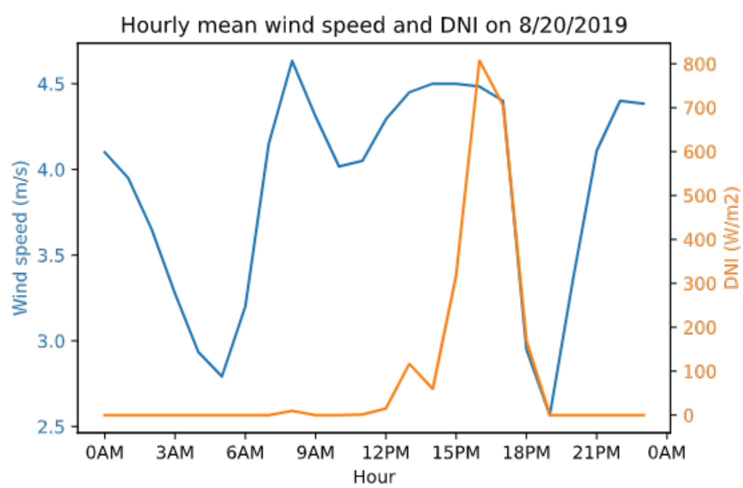

Figure 3.7: Interpolated wind speed and solar direct normal irradiance graph for a particular day

3.2.2 Geographic plots

For geographic visualization, the *energia.geo_plot()* is currently in development. It allows the user to visualize the geographic availability of a resource. For example, in fig. 3.8, availability of forest derived biomass for every county in the US is illustrated. Note that the counties wherein the availability is below a particular threshold are not represented. Other demographic attributes such as population can also be illustrated as shown in fig. 3.9.

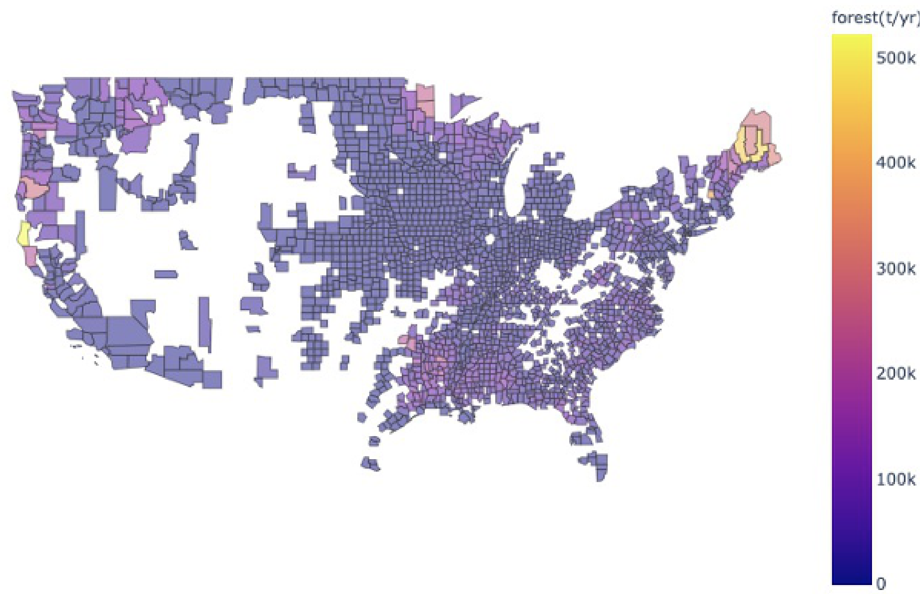

Figure 3.8: Geographic availability of forest derived biomass by county, US

3.3 Model reduction

3.3.1 Surrogate model approximation

The constituent process models in an energy system vary in complexity. Often, the models are nonlinear which can add significant complexity to the model formulation. Striking a balance between the rigor of these models and computational tractability can be a challenge. Moreover, the quality and validity of the optimal solutions depends on the quality and validity of the models

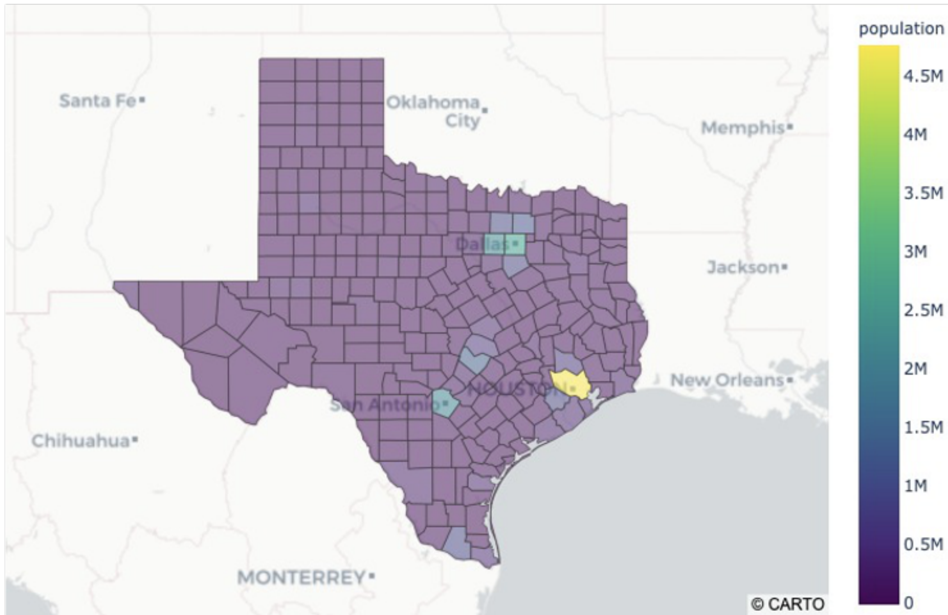

Figure 3.9: Population distribution by county, Texas

it involves. The main steps of surrogate model construction include experimental design, model selection, and model fitting.

Data-inspired surrogate models employ techniques such as regression, classification, interpolation, or artificial neural networks(ANN) [53, 54] and Rectified Linear Units (ReLU) [55] to avail of the theoretic and mechanistic insights provided by the governing mass, momentum, and energy balances. Data-driven modeling are particularly effective when a mechanistic understanding of the energy system is elusive or computationally prohibitive.

Hybrid models that incorporate concepts from both first principles and data driven approaches have become a mainstay in energy systems engineering as energy systems become more complex [56, 57, 58].

ENERGIA avails from embedded reduced order linear models prepared using the steady-state and dynamic models available in the model library, as also from open literature, to ensure that the model formulations are linear, thus ensuring optimality and convergence in feasible time.

3.3.2 Temporal clustering

At an hourly resolution, the number of data points for each attribute will be 8760. If implemented as part of comprehensive region-level mathematical formulation, the model can be computationally intractable. Various model reduction strategies have been suggested to address this. [59] proposed agglomerative hierarchical clustering (AHC) for contracting the time scale while still maintaining the chronological sequence of the data. The *energia.reduce_scenario()* function allows the user to define the method of choice as well as the number of clusters.

The *energia.reduce_scenario()* function itself relies on the mathematical functions such as the *energia.scaler()* which scales and reshapes the dataframe for the chosen attribute, the *energia.euclid()* function which calculates the euclidean distance between each cluster, and the *energia.generate_connectivity_matrix()* which generates a connectivity matrix to connect the data points within the cluster. Furthermore, *energia.reduce_scenario()* also provides a graphical representation of the clusters, the preservation of chronology in the case of AHC can be observed in the fig 3.10. Note that the output information is saved as a separate dataframe for ready access.

3.4 Integrated design, planning and scheduling

Individual constraints and objectives can be modeled using the pre-defined constraint and objective functions, and relational databases defined in ENERGIA. This includes a database of conversion parameters which requires the specification of process and resource as shown in fig 3.16, as also parameters for maximum storage and production capacity, resource availability, cost of purchase, cost of discharge, fixed and variable cost of operation and storage, transportation and storage losses.

3.4.1 Network synthesis

The constraints required for network synthesis can be implemented using the prototype by drawing from the exisiting values for maximum production and storage capacity. The constraints for the same are described below.

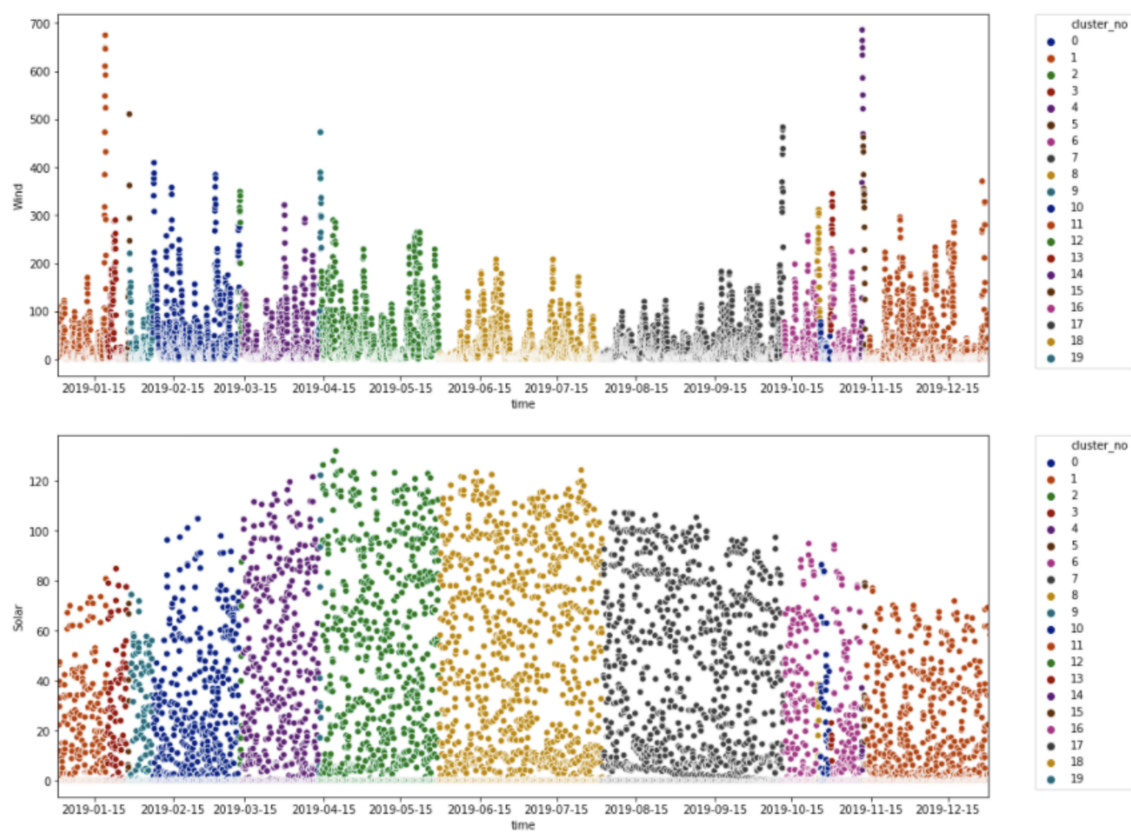

Figure 3.10: Wind and solar power potential clustered using agglomerative hierarchical clustering (AHC)

$$Cap_{a,i}^{P} \leq CAP_{i}^{P-max}.x_{a,i}^{P} \ \ \forall \ \ a \in \mathcal{A}, i \in \mathcal{I}$$

$$Cap_{a,j}^{S} \leq CAP_{i}^{S-max}.x_{a,j}^{S} \ \ \forall \ \ a \in \mathcal{A}, j \in \mathcal{J}$$

The software implementation of the constraints is shown in figs 3.11 and 3.12 respectively.

```
Cap_P[RS,AKE] - 100000*X_P[RS,AKE]  <=  0.0
```

Figure 3.11: Network design constraint for the setting up of a alkaline water electrolysis (AKE) unit in Amarillo, Texas

```
Cap_S[AM,CompressedH2] - 1000000000*X_S[AM,CompressedH2]  <=  0.0
```

Figure 3.12: Network design constraint for the setting up of a compressed hydrogen storage unit in Riverside, California

3.4.2 Integrated planning and scheduling

In a multi-location problem with two locations, 13 resources, and for annual operation, there will be a total of 22760 constraints wherein in the resource availability of each resource is limited to the maximum availability. Foremost, a relational database will need to be generated to store the parameters for each time period. This can be done using the *energia.make_B_max()* function. Additionally, the relational database can also be exported in the binary data form to be used on supercomputer clusters, the default *pickle* module on Python can be used for this purpose. The value for any location, resource, season (days in this case) and hour in the season can also be individually accessed as shown in fig 3.13. The constraint for the same time period is shown in 3.14. Constraints to determine time-varying production capacities can be implemented in ENERGIA.

```
B_MAX['AM']['Solar'][5][15]

110    43.756144
Name: Solar, dtype: float64
```

Figure 3.13: The maximum resource availability for solar power in Amarillo on day 5, at 15:00

Take the mass balance constraint for example:

$$B_{a,j,h,t} \leq B^{max}_{a,j,h,t} \ \ \forall \ \ a \in \mathcal{A}, j \in \mathcal{J}, h \in \mathcal{H}, t \in \mathcal{T}$$

The software implementation of the constraint is as shown below:

```
B[AM,Solar,5,15]  <=  43.756143758956874
```

Figure 3.14: Constraint for maximum resource availability for solar power in Amarillo on day 5, at 15:00

Similarly, general resource balance constraints that utilizes the conversion values can also be implemented as illustrated below:

$$Inv_{a,j,h,t} = (1 - LOSS_j).Inv_{a,j,h,t-1} + \sum_{\forall i \in \mathcal{I}} CONVERSION_{i,j}.P_{a,i,h,t} + B_{a,j,h,t} - S_{a,i,h,t}$$

3.4.3 Objective

Lastly, the objectives can be defined. For example, take the minimization objective of reducing the total annualized cost as shown below. Which can be implemented as shown in fig 3.17.

$$min \ \ Cost^{total} = 0.08.Capex^{total}_a + Opex^{total}_a \ \ \forall \ \ a \in \mathcal{A}$$

```
CONVERSION['AKE']['H2O']

-169.92
```

Figure 3.15: Conversion of water (H2O) using an alkaline water electrolysis (AKE)

```
Inv[RS,H2O,330,10] - (Inv[RS,H2O,330,9] - 169.92*P[RS,AKE,330,10] + B[RS,H2O,33
0,10] - S[RS,H2O,330,10])  ==  0.0
```

Figure 3.16: Resource balance constraint for water (H2O) in Riverside (RS)

```
0.08*Capex_total[AM] + Opex_total[AM] + 0.08*Capex_total[RS] + Opex_total[RS]
```

Figure 3.17: Objective for minimizing the total annualized cost of the system

As such, an entire energy system can be modeled with the choice of constraints being provided by the user. The system can then be optimized to the chosen objective of minimizing cost, maximizing production or utilization.

3.5 Solution and validation

The library of available models, their constituent process, energy feedstock and sources, transport options, and cost parameters can be used to formulate a mathematical programming model. For this purpose, ENERGIA uses the *pyomo* python [60, 61] module which allows the user the choice of solvers such as CPLEX [23], COIN-OR[62, 63], ipopt [64], and Gurobi [65] amongst others. Given the use of reduced order models and clustering of the temporal scale, solution validation becomes important. A paradigm to allow inline validation of the solutions is currently in development. The strategy relies on a library of steady-state and dynamic gPROMS simulations. This will allow users to ascertain both the validity and accuracy of the solution in real time.

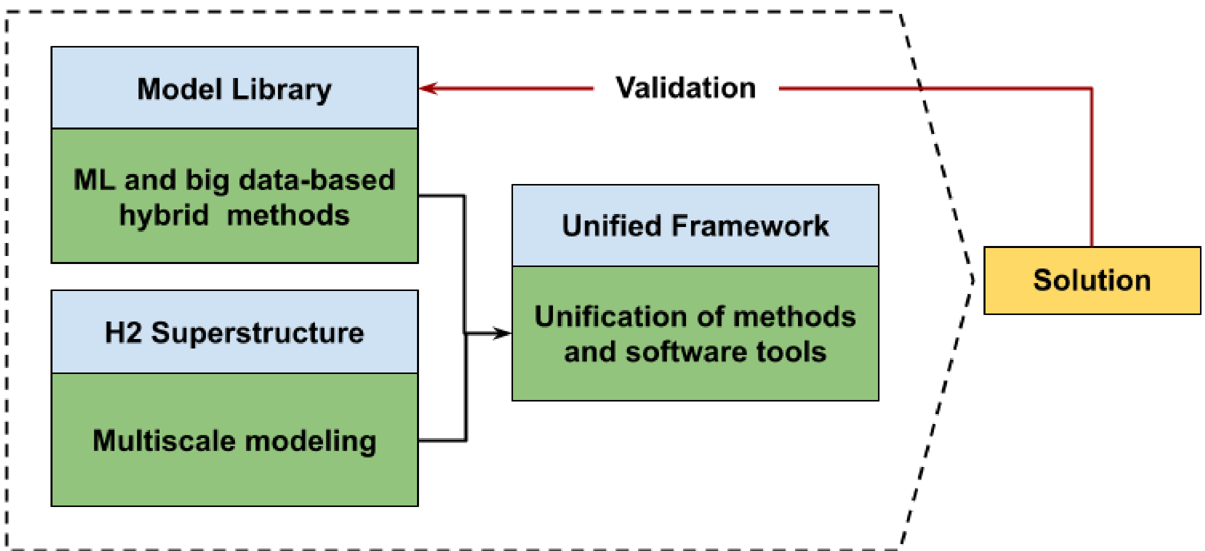

Figure 3.18: Validation of solutions

4. SUMMARY AND FURTHER STUDY

In the presented work, the various capabilities of ENERGIA are highlighted. Firstly, methods to acquire location based data from various publicly available databases are shown. The data can be used to form data structures which allow for statistical analyses using the many open-source Python modules. The data is on both the temporal and geographic scale. Temporal resolution can be chosen by the user to a minimum of five minute intervals. Geographic data is at a county level resolution. Temporal data includes weather related, and time variant resource availability. Geographic data such as the availability of various biomass alternatives, available areas, and methane emission from various sources can also be accessed through the prototype. ENERGIA stores the large amount of data in the form of relational databases. Methods to access individual data points at a location, for a particular resource or process, in a given season and hour are elucidated.

The varied visualization capabilities of ENERGIA are demonstrated. The visualization functions allow the user to define the temporal and geographic resolution. The availability for a particular resource, for example, can be illustrated on both a chosen temporal or a geographic scale. This allows users to visualize the problem and develop a suitable strategy to implement a mathematical formulation of the energy system. Moreover, statistical functions for clustering can be used for model reduction allowing the potential reduction of computational expense and time.

An important potential feature in ENERGIA is a strategy to allow in-line validation of solution using a library of cross-platform dynamic and steady-state simulation models curated to represent the key processes inherent to future energy systems.

Values such as maximum production and storage capacities, piece-wise costing functions, and conversion parameters are embedded in the system. Users can pull data from the relational databases and embedded data to form constraints and objectives to define a full scale model. The formulation of such constraints and objectives is also demonstrated. The formulated model can be subsequently solved using the solvers.

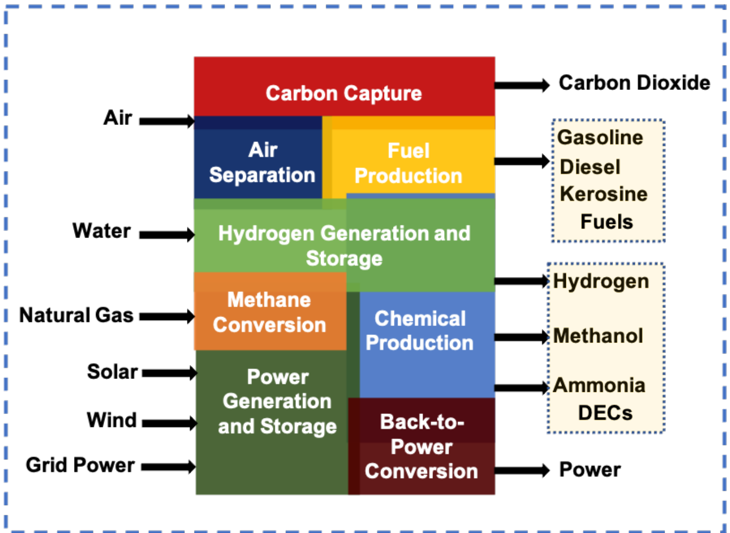

Figure 4.1: Constituent processes in a multi-product energy systems

4.1 Further Study

The prototype will be first expanded to included mode based constraints, and time-variant costing data, and accurate process parameters. This will allows the implementation of a full scale model to resolve a hydrogen supply chain for the utilization of the renewable potential of California and Texas to meet the energy demand for transportation in California with the scope of supplying energy to geographically distant places through the ports in California. The parameters and modes for transportation will be defined to utilize to the fullest extent the existing transportation infrastructure.

The solution methodology will be expanded to implement the recent works in heuristics by Allen et. al. [10], as also the effects of carbon credits and cost to consumer as presented in the recent works by Baratsas et. al. [4, 66]. Moreover, a comprehensive model library consisting of biomass, natural gas, and renewable process will be appended to the prototype to allow users to develop comprehensive energy system formulations.

The prototype will also eventually allow for piece-wise linearization functions, and machine learning and neural network based model reduction techniques. A comprehensive validation methodology will also be developed.

REFERENCES

[1] R. Kakodkar, G. He, C. Demirhan, M. Arbabzadeh, S. Baratsas, S. Avraamidou, D. Mallapragada, I. Miller, R. Allen, E. Gençer, and E. Pistikopoulos, "A review of analytical and optimization methodologies for transitions in multi-scale energy systems." submitted manuscript, 2021.

[2] E. Gençer, S. Torkamani, I. Miller, T. W. Wu, and F. O'Sullivan, "Sustainable energy system analysis modeling environment: Analyzing life cycle emissions of the energy transition," *Applied Energy*, vol. 277, p. 115550, 2020.

[3] A. Werner, G. A. Perez-Valdes, U. Johansen, and A. Stokka, "Remes-a regional equilibrium model for norway with focus on the energy system," *SINTEF Rapport*, 2017.

[4] S. G. Baratsas, A. M. Niziolek, O. Onel, L. R. Matthews, C. A. Floudas, D. R. Hallermann, S. M. Sorescu, and E. N. Pistikopoulos, "A framework to predict the price of energy for the end-users with applications to monetary and energy policies," *Nature Communications*, vol. 12, no. 1, 2021.

[5] C. D. Demirhan, F. Boukouvala, K. Kim, H. Song, W. W. Tso, C. A. Floudas, and E. N. Pistikopoulos, "An integrated data-driven modeling global optimization approach for multi-period nonlinear production planning problems," *Computers Chemical Engineering*, vol. 141, p. 107007, 2020.

[6] W. W. Tso, C. D. Demirhan, C. A. Floudas, and E. N. Pistikopoulos, "Multi-scale energy systems engineering for optimal natural gas utilization," *Catalysis Today*, vol. 356, p. 18–26, 2020.

[7] C. D. Demirhan, W. W. Tso, J. B. Powell, C. F. Heuberger, and E. N. Pistikopoulos, "A multiscale energy systems engineering approach for renewable power generation and storage optimization," *Industrial Engineering Chemistry Research*, vol. 59, no. 16, p. 7706–7721, 2020.

[8] M. J. Palys, H. Wang, Q. Zhang, and P. Daoutidis, "Renewable ammonia for sustainable energy and agriculture: vision and systems engineering opportunities," *Current Opinion in Chemical Engineering*, vol. 31, p. 100667, 2021.

[9] (IRENA), "Renewable capacity statistics 2021 international renewable energy agency," 2021.

[10] R. C. Allen, S. G. Baratsas, R. Kakodkar, S. Avraamidou, J. B. Powell, C. F. Heuberger, C. D. Demirhan, and E. N. Pistikopoulos, "Optimization framework for solving integrated planning and scheduling problems for dense energy carriers," *Proceedings of the 11th IFAC International Symposium on Advanced Control of Chemical Processes*, 2021.

[11] M. Meinshausen, N. Meinshausen, W. Hare, S. C. B. Raper, K. Frieler, R. Knutti, D. J. Frame, and M. R. Allen, "Greenhouse-gas emission targets for limiting global warming to 2°c," *Nature*, vol. 458, no. 7242, p. 1158–1162, 2009.

[12] H. Ritchie and D. S. Reay, "Delivering the two degree global climate change target using a flexible ratchet framework," *Climate Policy*, vol. 17, no. 8, p. 1031–1045, 2017.

[13] J. Rogelj, D. Shindell, K. Jiang, S. Fifita, P. Forster, V. Ginzburg, C. Handa, H. Kheshgi, S. Kobayashi, E. Kriegler, L. Mundaca, R. Séférian, and t. . M. y. . . Vilariño, M.V.

[14] Royal Dutch Shell, "SKY Scenario." `https://www.shell.com/energy-and-innovation/the-energy-future/scenarios/shell-scenario-sky.html`, 2018.

[15] R. Loulou, G. Goldstein, K. Noble, *et al.*, "Documentation for the markal family of models," *Energy Technology Systems Analysis Programme*, pp. 65–73, 2004.

[16] D. Finon, "Optimisation model for the french energy sector," *Energy Policy*, vol. 2, no. 2, p. 136–151, 1974.

[17] E. Van Der Voort, "The efom 12c energy supply model within the ec modelling system," *Omega*, vol. 10, no. 5, p. 507–523, 1982.

[18] J. Bisschop and A. Meeraus, “On the Development of a General Algebraic Modeling System in a Strategic Planning Environment,” in *Applications*, vol. 20 of *Mathematical Programming Studies*, pp. 1–29, Springer Berlin Heidelberg, 1982.

[19] GAMS Development Corporation, Washington, DC, USA, *GAMS - A User’s Guide, GAMS Release 24.2.1*, 2013.

[20] R. Kannan, N. Strachan, G. Anandarajah, and B. Ozkan, “Uk markal model documentation,” 2007.

[21] H. d. Kruijk, “The eu energy and environmental model efom-env specified in gams. model description and user’s guide.,” *Policy Studies*, vol. 2012, p. 2011, 2013.

[22] R. Loulou and M. Labriet, “Etsap-tiam: the times integrated assessment model part i: Model structure,” *Computational Management Science*, vol. 5, no. 1-2, p. 7–40, 2008.

[23] I. I. Cplex, “V12. 1: User’s manual for cplex,” *International Business Machines Corporation*, vol. 46, no. 53, p. 157, 2009.

[24] K. Poncelet, E. Delarue, D. Six, J. Duerinck, and W. D’Haeseleer, “Impact of the level of temporal and operational detail in energy-system planning models,” *Applied Energy*, vol. 162, p. 631–643, 2016.

[25] H.-K. Ringkjøb, P. M. Haugan, and I. M. Solbrekke, “A review of modelling tools for energy and electricity systems with large shares of variable renewables,” *Renewable and Sustainable Energy Reviews*, vol. 96, p. 440–459, 2018.

[26] Energy Exemplar, “AURORA Electric Modeling Forecasting and Analysis Software.” `https://energyexemplar.com/products/aurora-electric-modeling-forecasting-software/`.

[27] W.-P. Schill and A. Zerrahn, “Long-run power storage requirements for high shares of renewables: Results and sensitivities,” *Renewable and Sustainable Energy Reviews*, vol. 83, p. 156–171, 2018.

[28] A. Zerrahn and W.-P. Schill, “Long-run power storage requirements for high shares of renewables: review and a new model,” *Renewable and Sustainable Energy Reviews*, vol. 79, p. 1518–1534, 2017.

[29] F. Wiese, R. Bramstoft, H. Koduvere, A. Pizarro Alonso, O. Balyk, J. G. Kirkerud, G. Tveten, T. F. Bolkesjø, M. Münster, H. Ravn, and et al., “Balmorel open source energy system model,” *Energy Strategy Reviews*, vol. 20, p. 26–34, 2018.

[30] C. F. Heuberger, E. S. Rubin, I. Staffell, N. Shah, and N. Mac Dowell, “Power capacity expansion planning considering endogenous technology cost learning,” *Applied Energy*, vol. 204, p. 831–845, 2017.

[31] California Energy Commission, “Solar Energy Projects in California.” `https://ww2.energy.ca.gov/sitingcases/solar/index_cms.html`, 2021.

[32] NREL, “Energy Atlas,”

[33] U. C. Bureau, “2010 Census of Population and Housing, Population and Housing Unit Counts, CPH-2-5. U.S. ,” 2012.

[34] D. Nunez, “AB-32 Air pollution: greenhouse gases: California Global Warming Solutions Act of 2006.,”

[35] E. G. Brown Jr., “Executive Order B-30-15,”

[36] E. G. Brown Jr., “Executive Order B-55-18,”

[37] F. Pavley, “SB-32 California Global Warming Solutions Act of 2006: emissions limit.,”

[38] F. Pavley, “AB-1493 Vehicular emissions: greenhouse gases,”

[39] D. Steinberg, “SB-375 Transportation planning: travel demand models: sustainable communities strategy: environmental review.,”

[40] W. Chesbro, “AB-341 Solid waste: diversion.,”

[41] K. De León, “SB-535 California Global Warming Solutions Act of 2006: Greenhouse Gas Reduction Fund.,”

[42] C. E. Commission, "CEC-1304 QFER Database,"

[43] U. E. I. Administration, "Texas - State Profile and Energy Estimates,"

[44] U. E. I. Administration, "Texas Natural Gas Marketed Production,"

[45] A. M. Mroue, R. H. Mohtar, E. N. Pistikopoulos, and M. T. Holtzapple, "Energy portfolio assessment tool (epat): Sustainable energy planning using the wef nexus approach – texas case," *Science of The Total Environment*, vol. 648, p. 1649–1664, 2019.

[46] U. E. I. Administration, "Today in Energy,"

[47] C. Bell, "HB 4472 Relating to the Texas emissions reduction plan.,"

[48] Office of the Texas Governor, Greg Abbott, "Governor Abbott Signs ERCOT Reforms, Power Grid Weatherization Legislation Into Law."

[49] E. B. Johnson, "H.R.34 - Energy and Water Research Integration Act of 2019.,"

[50] G. S. Ogumerem and E. N. Pistikopoulos, "Parametric optimization and control toward the design of a smart metal hydride refueling system," *AIChE Journal*, vol. 65, no. 10, p. e16680, 2019.

[51] Kawasaki Heavy Industries Ltd., "World's First Liquefied Hydrogen Carrier SUISO FRONTIER Launches Building an International Hydrogen Energy Supply Chain Aimed at Carbon-free Society." `https://global.kawasaki.com/en/corp/newsroom/news/detail/?f=20191211_3487`, 2019.

[52] W. F. Holmgren, C. W. Hansen, and M. A. Mikofski, "pvlib python: a python package for modeling solar energy systems," *Journal of Open Source Software*, vol. 3, no. 29, p. 884, 2018.

[53] B. Wang, B. Xie, J. Xuan, and K. Jiao, "Ai-based optimization of pem fuel cell catalyst layers for maximum power density via data-driven surrogate modeling," *Energy Conversion and Management*, vol. 205, p. 112460, 2020.

[54] A. H. Elsheikh, S. W. Sharshir, M. Abd Elaziz, A. Kabeel, W. Guilan, and Z. Haiou, "Modeling of solar energy systems using artificial neural network: A comprehensive review," *Solar Energy*, vol. 180, p. 622–639, 2019.

[55] B. Grimstad and H. Andersson, "Relu networks as surrogate models in mixed-integer linear programs," *Computers Chemical Engineering*, vol. 131, p. 106580, 2019.

[56] B. Beykal, F. Boukouvala, C. A. Floudas, and E. N. Pistikopoulos, "Optimal design of energy systems using constrained grey-box multi-objective optimization," *Computers & Chemical Engineering*, vol. 116, p. 488–502, 2018.

[57] M. S. F. Bangi and J. S.-I. Kwon, "Deep hybrid modeling of chemical process: Application to hydraulic fracturing," *Computers Chemical Engineering*, vol. 134, p. 106696, 2020.

[58] G. Zahedi, A. Lohi, and K. Mahdi, "Hybrid modeling of ethylene to ethylene oxide heterogeneous reactor," *Fuel Processing Technology*, vol. 92, no. 9, p. 1725–1732, 2011.

[59] W. W. Tso, C. D. Demirhan, C. F. Heuberger, J. B. Powell, and E. N. Pistikopoulos, "A hierarchical clustering decomposition algorithm for optimizing renewable power systems with storage," *Applied Energy*, vol. 270, p. 115190, 2020.

[60] W. E. Hart, J.-P. Watson, and D. L. Woodruff, "Pyomo: modeling and solving mathematical programs in python," *Mathematical Programming Computation*, vol. 3, no. 3, pp. 219–260, 2011.

[61] M. L. Bynum, G. A. Hackebeil, W. E. Hart, C. D. Laird, B. L. Nicholson, J. D. Siirola, J.-P. Watson, and D. L. Woodruff, *Pyomo–optimization modeling in python*, vol. 67. Springer Science & Business Media, third ed., 2021.

[62] T. Hothorn, K. Hornik, M. A. van de Wiel, and A. Zeileis, "A Lego system for conditional inference," *The American Statistician*, vol. 60, no. 3, pp. 257–263, 2006.

[63] T. Hothorn, K. Hornik, M. A. van de Wiel, and A. Zeileis, "Implementing a class of permutation tests: The coin package," *Journal of Statistical Software*, vol. 28, no. 8, pp. 1–23, 2008.

[64] A. Wächter and L. T. Biegler, "On the implementation of a primal-dual interior point filter line search algorithm for large-scale nonlinear programming," *Mathematical Programming*, vol. 106, no. 1, pp. 25–57, 2006.

[65] L. Gurobi Optimization, "Gurobi optimizer reference manual," 2021.

[66] S. G. Baratsas, A. M. Niziolek, O. Onel, L. R. Matthews, C. A. Floudas, D. R. Hallermann, S. M. Sorescu, and E. N. Pistikopoulos, "A framework to predict the price of energy for the end-users with applications to monetary and energy policies," *Nature Communications*, vol. 12, p. 18, jan 2021.

[67] United Nations, Department of Economic and Social Affairs, Population Division, "World Population Prospects." `https://population.un.org`, 2019.

[68] B. Johnson, "Energy and Civilization: A History. By Vaclav Smil," *Environmental History*, vol. 23, pp. 658–659, 05 2018.

[69] "AR5 Climate Change 2014: Mitigation of Climate Change," *IPCC*, 2014.

[70] M. Child, D. Bogdanov, and C. Breyer, "The role of storage technologies for the transition to a 100% renewable energy system in europe," *Energy Procedia*, vol. 155, p. 44–60, 2018.

[71] T. Brown, D. Schlachtberger, A. Kies, S. Schramm, and M. Greiner, "Synergies of sector coupling and transmission reinforcement in a cost-optimised, highly renewable european energy system," *Energy*, vol. 160, p. 720–739, 2018.

[72] "Rethinking energy 2017: Accelerating the global energy transformation," *IRENA*, 2017.

[73] M. Mehos, H. Price, R. Cable, D. Kearney, B. Kelly, G. Kolb, and F. Morse, "Concentrating solar power best practices study," 2020.

[74] D. Pudjianto, M. Aunedi, P. Djapic, and G. Strbac, "Whole-systems assessment of the value of energy storage in low-carbon electricity systems," *IEEE Transactions on Smart Grid*, vol. 5, no. 2, p. 1098–1109, 2014.

[75] R. C. Pietzcker, F. Ueckerdt, S. Carrara, H. S. De Boer, J. Després, S. Fujimori, N. Johnson, A. Kitous, Y. Scholz, P. Sullivan, and et al., "System integration of wind and solar power in integrated assessment models: A cross-model evaluation of new approaches," *Energy Economics*, vol. 64, p. 583–599, 2017.

[76] P. Liu, M. C. Georgiadis, and E. N. Pistikopoulos, "Advances in energy systems engineering," *Industrial Engineering Chemistry Research*, vol. 50, no. 9, p. 4915–4926, 2011.

[77] B. K. Sovacool, "How long will it take? conceptualizing the temporal dynamics of energy transitions," *Energy Research Social Science*, vol. 13, p. 202–215, 2016.

[78] A. J. Chapman and K. Itaoka, "Energy transition to a future low-carbon energy society in japan's liberalizing electricity market: Precedents, policies and factors of successful transition," *Renewable and Sustainable Energy Reviews*, vol. 81, p. 2019–2027, 2018.

[79] C. D. Demirhan, W. W. Tso, G. S. Ogumerem, and E. N. Pistikopoulos, "Energy systems engineering - a guided tour," *BMC Chemical Engineering*, vol. 1, no. 1, p. 11, 2019.

[80] D. o. E. United Nations and S. D. Social Affairs, "The 2030 agenda for sustainable development," 2013.

[81] E. A. Olivetti, G. Ceder, G. G. Gaustad, and X. Fu, "Lithium-ion battery supply chain considerations: Analysis of potential bottlenecks in critical metals," *Joule*, vol. 1, no. 2, p. 229–243, 2017.

[82] S. Avraamidou, S. G. Baratsas, Y. Tian, and E. N. Pistikopoulos, "Circular economy-a challenge and an opportunity for process systems engineering," *Computers & Chemical Engineering*, vol. 133, p. 106629, 2020.

[83] P. Maheshwari, S. Singla, and Y. Shastri, "Resiliency optimization of biomass to biofuel supply chain incorporating regional biomass pre-processing depots," *Biomass and Bioenergy*, vol. 97, p. 116–131, 2017.

[84] M. Aalto, O. Korpinen, T. Ranta, *et al.*, "Feedstock availability and moisture content data processing for multi-year simulation of forest biomass supply in energy production," *Silva Fenn*, vol. 53, 2019.

[85] C. Kelliher and D. Anderson, "Doing more with less? flexible working practices and the intensification of work," *Human Relations*, vol. 63, no. 1, p. 83–106, 2010.

[86] G. Ruan, D. Wu, X. Zheng, H. Zhong, C. Kang, M. A. Dahleh, S. Sivaranjani, and L. Xie, "A cross-domain approach to analyzing the short-run impact of covid-19 on the us electricity sector," *Joule*, vol. 4, no. 11, p. 2322–2337, 2020.

[87] Z. Zhang, A. Arshad, C. Zhang, S. Hussain, and W. Li, "Unprecedented temporary reduction in global air pollution associated with covid-19 forced confinement: A continental and city scale analysis," *Remote Sensing*, vol. 12, no. 15, p. 2420, 2020.

[88] V. Dua and E. N. Pistikopoulos, "None," *Annals of Operations Research*, vol. 99, no. 1/4, p. 123–139, 2000.

[89] C. S. Adjiman, I. P. Androulakis, and C. A. Floudas, "Global optimization of mixed-integer nonlinear problems," *AIChE Journal*, vol. 46, no. 9, p. 1769–1797, 2000.

[90] J. Rogelj, M. Den Elzen, N. Höhne, T. Fransen, H. Fekete, H. Winkler, R. Schaeffer, F. Sha, K. Riahi, M. Meinshausen, and et al., "Paris agreement climate proposals need a boost to keep warming well below 2°c," *Nature*, vol. 534, no. 7609, p. 631–639, 2016.

[91] P. IEA, "World energy outlook," 2020.

[92] E. I. Agency, "Monthly energy review - april," 2020.

[93] D. Nugent and B. K. Sovacool, "Assessing the lifecycle greenhouse gas emissions from solar pv and wind energy: A critical meta-survey," *Energy Policy*, vol. 65, p. 229–244, 2014.

[94] B. M. Rule, Z. J. Worth, and C. A. Boyle, "Comparison of life cycle carbon dioxide emissions and embodied energy in four renewable electricity generation technologies in new zealand," *Environmental Science Technology*, vol. 43, no. 16, p. 6406–6413, 2009.

[95] R. Turconi, A. Boldrin, and T. Astrup, "Life cycle assessment (lca) of electricity generation technologies: Overview, comparability and limitations," *Renewable and Sustainable Energy Reviews*, vol. 28, p. 555–565, 2013.

[96] S. S. Ahmad, F. S. Al-Ismail, A. A. Almehizia, and M. Khalid, "Model predictive control approach for optimal power dispatch and duck curve handling under high photovoltaic power penetration," *IEEE Access*, vol. 8, p. 186840–186850, 2020.

[97] L. A. Wong, V. K. Ramachandaramurthy, S. L. Walker, and J. B. Ekanayake, "Optimal placement and sizing of battery energy storage system considering the duck curve phenomenon," *IEEE Access*, vol. 8, p. 197236–197248, 2020.

[98] M. Sheha, K. Mohammadi, and K. Powell, "Solving the duck curve in a smart grid environment using a non-cooperative game theory and dynamic pricing profiles," *Energy Conversion and Management*, vol. 220, p. 113102, 2020.

[99] P. L. Joskow, "Transmission capacity expansion is needed to decarbonize the electricity sector efficiently," *Joule*, vol. 4, no. 1, p. 1–3, 2020.

[100] H. X. Li, D. J. Edwards, M. R. Hosseini, and G. P. Costin, "A review on renewable energy transition in australia: An updated depiction," *Journal of Cleaner Production*, vol. 242, p. 118475, 2020.

[101] A. Boretti, "Production of hydrogen for export from wind and solar energy, natural gas, and coal in australia," *International Journal of Hydrogen Energy*, vol. 45, no. 7, p. 3899–3904, 2020.

[102] F. I. Gallardo, A. Monforti Ferrario, M. Lamagna, E. Bocci, D. Astiaso Garcia, and T. E. Baeza-Jeria, "A techno-economic analysis of solar hydrogen production by electrolysis in the north of chile and the case of exportation from atacama desert to japan," *International Journal of Hydrogen Energy*, 2020.

[103] D. J. Garcia and F. You, "The water-energy-food nexus and process systems engineering: A new focus," *Computers Chemical Engineering*, vol. 91, pp. 49 – 67, 2016. 12th Inter-

national Symposium on Process Systems Engineering 25th European Symposium of Computer Aided Process Engineering (PSE-2015/ESCAPE-25), 31 May - 4 June 2015, Copenhagen, Denmark.

[104] Y. Nie, S. Avraamidou, X. Xiao, E. N. Pistikopoulos, J. Li, Y. Zeng, F. Song, J. Yu, and M. Zhu, "A food-energy-water nexus approach for land use optimization," *Science of The Total Environment*, vol. 659, pp. 7 – 19, 2019.

[105] Y. Nie, S. Avraamidou, J. Li, X. Xiao, and E. N. Pistikopoulos, "Land use modeling and optimization based on food-energy-water nexus: a case study on crop-livestock systems," in *13th International Symposium on Process Systems Engineering (PSE 2018)* (M. R. Eden, M. G. Ierapetritou, and G. P. Towler, eds.), vol. 44 of *Computer Aided Chemical Engineering*, pp. 1939 – 1944, Elsevier, 2018.

[106] M. Arthur, G. Liu, Y. Hao, L. Zhang, S. Liang, E. F. Asamoah, and G. V. Lombardi, "Urban food-energy-water nexus indicators: A review," *Resources Conservation and Recycling*, vol. 151, p. 104481, 2019.

[107] H. K. Jeswani, R. Burkinshaw, and A. Azapagic, "Environmental sustainability issues in the food–energy–water nexus: Breakfast cereals and snacks," *Sustainable Production and Consumption*, vol. 2, p. 17–28, 2015.

[108] J. Sherwood, R. Clabeaux, and M. Carbajales-Dale, "An extended environmental input–output lifecycle assessment model to study the urban food–energy–water nexus," *Environmental Research Letters*, vol. 12, no. 10, p. 105003, 2017.

[109] K. M. Kibler, D. Reinhart, C. Hawkins, A. M. Motlagh, and J. Wright, "Food waste and the food-energy-water nexus: A review of food waste management alternatives," *Waste Management*, vol. 74, p. 52–62, 2018.

[110] R. C. Allen, Y. Nie, S. Avraamidou, and E. N. Pistikopoulos, "Infrastructure planning and operational scheduling for power generating systems: An energy-water nexus approach," in *Proceedings of the 9th International Conference on Foundations of Computer-Aided Process*

Design (S. G. Muñoz, C. D. Laird, and M. J. Realff, eds.), vol. 47 of *Computer Aided Chemical Engineering*, pp. 233 – 238, Elsevier, 2019.

[111] S. Avraamidou, A. Milhorn, O. Sarwar, and E. N. Pistikopoulos, "Towards a quantitative food-energy-water nexus metric to facilitate decision making in process systems: A case study on a dairy production plant," in *28th European Symposium on Computer Aided Process Engineering* (A. Friedl, J. J. Klemeš, S. Radl, P. S. Varbanov, and T. Wallek, eds.), vol. 43 of *Computer Aided Chemical Engineering*, pp. 391 – 396, Elsevier, 2018.

[112] Ellen MacArthur Foundation (EMF), "Circularity indicators: An approach to measuring circularity—Methodology," 2015.

[113] T. Ramachandra and B. Shruthi, "Spatial mapping of renewable energy potential," *Renewable and Sustainable Energy Reviews*, vol. 11, no. 7, pp. 1460 – 1480, 2007.

[114] K. Kaygusuz and A. Sarı, "Renewable energy potential and utilization in turkey," *Energy Conversion and Management*, vol. 44, no. 3, p. 459–478, 2003.

[115] J. Kosowatz, "Energy storage smooths the duck curve," *Mechanical Engineering*, vol. 140, no. 06, p. 30–35, 2018.

[116] S. Ould Amrouche, D. Rekioua, T. Rekioua, and S. Bacha, "Overview of energy storage in renewable energy systems," *International Journal of Hydrogen Energy*, vol. 41, no. 45, p. 20914–20927, 2016.

[117] H. Lund and G. Salgi, "The role of compressed air energy storage (caes) in future sustainable energy systems," *Energy Conversion and Management*, vol. 50, no. 5, p. 1172–1179, 2009.

[118] Y.-C. Tsai, Y.-K. Chan, F.-K. Ko, and J.-T. Yang, "Integrated operation of renewable energy sources and water resources," *Energy Conversion and Management*, vol. 160, p. 439–454, 2018.

[119] J. Jurasz, "Modeling and forecasting energy flow between national power grid and a solar–wind–pumped-hydroelectricity (pv–wt–psh) energy source," *Energy Conversion and Management*, vol. 136, p. 382–394, 2017.

[120] G. S. Ogumerem, W. W. Tso, C. D. Demirhan, S. Y. Lee, H. E. Song, and E. N. Pistikopoulos, “Toward the optimization of hydrogen, ammonia, and methanol supply chains,” *IFAC-PapersOnLine*, vol. 52, no. 1, p. 844–849, 2019.

[121] D. S. Mallapragada, N. A. Sepulveda, and J. D. Jenkins, “Long-run system value of battery energy storage in future grids with increasing wind and solar generation,” *Applied Energy*, vol. 275, p. 115390, 2020.

[122] R. S. Go, F. D. Munoz, and J.-P. Watson, “Assessing the economic value of co-optimized grid-scale energy storage investments in supporting high renewable portfolio standards,” *Applied Energy*, vol. 183, p. 902–913, 2016.

[123] O. of Energy Efficiency & Renewable Energy (US), “Pumped-storage hydropower.”

[124] H. Nishide, K. Koshika, and K. Oyaizu, “Environmentally benign batteries based on organic radical polymers,” *Pure and Applied Chemistry*, vol. 81, no. 11, p. 1961–1970, 2009.

[125] X. Wu, Y. Cao, X. Ai, J. Qian, and H. Yang, “A low-cost and environmentally benign aqueous rechargeable sodium-ion battery based on nati2(po4)3–na2nife(cn)6 intercalation chemistry,” *Electrochemistry Communications*, vol. 31, p. 145–148, 2013.

[126] T. Chen, Y. Jin, H. Lv, A. Yang, M. Liu, B. Chen, Y. Xie, and Q. Chen, “Applications of lithium-ion batteries in grid-scale energy storage systems,” *Transactions of Tianjin University*, vol. 26, no. 3, p. 208–217, 2020.

[127] M. Ling, H. Zhao, X. Xiaoc, F. Shi, M. Wu, J. Qiu, S. Li, X. Song, G. Liu, S. Zhang, and et al., “Low cost and environmentally benign crack-blocking structures for long life and high power si electrodes in lithium ion batteries,” *Journal of Materials Chemistry A*, vol. 3, no. 5, p. 2036–2042, 2015.

[128] H. Xu, L. Guo, H. Tian, and C. Pan, “Thermodynamic optimization of water-cooled infrastructure for vehicle lithium–ion battery based on exergy,” *Journal of Thermophysics and Heat Transfer*, vol. 34, no. 2, pp. 304–313, 2020.

[129] S. F. Lux, F. Schappacher, A. Balducci, S. Passerini, and M. Winter, "Low cost, environmentally benign binders for lithium-ion batteries," *Journal of the Electrochemical Society*, vol. 157, no. 3, p. A320, 2010.

[130] J. F. Peters, M. Baumann, B. Zimmermann, J. Braun, and M. Weil, "The environmental impact of li-ion batteries and the role of key parameters – a review," *Renewable and Sustainable Energy Reviews*, vol. 67, p. 491–506, 2017.

[131] B. L. Ellis and L. F. Nazar, "Sodium and sodium-ion energy storage batteries," *Current Opinion in Solid State and Materials Science*, vol. 16, no. 4, p. 168–177, 2012.

[132] C. Delmas, "Sodium and sodium-ion batteries: 50 years of research," *Advanced Energy Materials*, vol. 8, no. 17, p. 1703137, 2018.

[133] D. H. P. Kang, M. Chen, and O. A. Ogunseitan, "Potential environmental and human health impacts of rechargeable lithium batteries in electronic waste," *Environmental Science Technology*, vol. 47, no. 10, p. 5495–5503, 2013.

[134] M. Chen, X. Ma, B. Chen, R. Arsenault, P. Karlson, N. Simon, and Y. Wang, "Recycling end-of-life electric vehicle lithium-ion batteries," *Joule*, vol. 3, no. 11, pp. 2622–2646, 2019.

[135] M. Arbabzadeh, G. M. Lewis, and G. A. Keoleian, "Green principles for responsible battery management in mobile applications," *Journal of Energy Storage*, vol. 24, p. 100779, 2019.

[136] I. Dincer and C. Acar, "Review and evaluation of hydrogen production methods for better sustainability," *International Journal of Hydrogen Energy*, vol. 40, no. 34, p. 11094–11111, 2015.

[137] F. Barbir, "Pem electrolysis for production of hydrogen from renewable energy sources," *Solar Energy*, vol. 78, no. 5, p. 661–669, 2005.

[138] J. D. Fonseca, M. Camargo, J.-M. Commenge, L. Falk, and I. D. Gil, "Trends in design of distributed energy systems using hydrogen as energy vector: A systematic literature review," *International Journal of Hydrogen Energy*, vol. 44, no. 19, p. 9486–9504, 2019.

[139] H. Nami, F. Mohammadkhani, and F. Ranjbar, "Utilization of waste heat from gtmhr for hydrogen generation via combination of organic rankine cycles and pem electrolysis," *Energy Conversion and Management*, vol. 127, p. 589–598, 2016.

[140] B. Gaudernack and S. Lynum, "Hydrogen from natural gas without release of co2 to the atmosphere," *International Journal of Hydrogen Energy*, vol. 23, no. 12, p. 1087–1093, 1998.

[141] A. Valera-Medina, H. Xiao, M. Owen-Jones, W. David, and P. Bowen, "Ammonia for power," *Progress in Energy and Combustion Science*, vol. 69, p. 63–102, 2018.

[142] D. Brown, "Us hydrogen production–2015," *CryoGas International*, 2016.

[143] C. D. Demirhan, W. W. Tso, J. B. Powell, and E. N. Pistikopoulos, "Sustainable ammonia production through process synthesis and global optimization," *AIChE Journal*, vol. 65, no. 7, p. e16498, 2019.

[144] R. M. Nayak-Luke and R. Bañares-Alcántara, "Techno-economic viability of islanded green ammonia as a carbon-free energy vector and as a substitute for conventional production," *Energy Environmental Science*, vol. 13, no. 9, p. 2957–2966, 2020.

[145] OECD, *Taxing Energy Use 2019: Using Taxes for Climate Action*. OECD Publishing, 2019.

[146] M. A. Pigato, *Fiscal Policies for Development and Climate Action*. The World Bank, 2018.

[147] I. W. Parry, M. D. Heine, E. Lis, and S. Li, *Getting energy prices right: From principle to practice*. International Monetary Fund, 2014.

[148] International Monetary Fund, "Fiscal Monitor: How to Mitigate Climate Change," tech. rep., Washington, DC, USA, October 2019.

[149] Postic, Sébastien and Fetet, Marion, "Global Carbon Accounts 2020." `https://www.i4ce.org/wp-core/wp-content/uploads/2020/05/TarificationCarbone2020-VA.pdf`, 2020.

[150] W. Bank, "State and trends of carbon pricing 2020," *World Bank Publications, Washington, DC*, 2020.

[151] Edmonds, Jae and Forrister, Dirk and Clarke, Leon and de Clara, Stefano and Munnings, Clayton, "The economic potential of article 6 of the Paris Agreement and implementation challenges," 2019.

[152] Intergovernmental Panel on Climate Change (IPCC), "Global Warming of 1.5°C."

[153] A. Ciroth, "Ict for environment in life cycle applications openlca—a new open source software for life cycle assessment," *The International Journal of Life Cycle Assessment*, vol. 12, no. 4, p. 209, 2007.

[154] I. T. Herrmann and A. Moltesen, "Does it matter which life cycle assessment (lca) tool you choose?–a comparative assessment of simapro and gabi," *Journal of Cleaner Production*, vol. 86, pp. 163–169, 2015.

[155] PRé Sustainability, "Manual: SimaPro Tutorial n.d.." `https://support.simapro.com/articles/Manual/SimaPro-Tutorial/?l=en_US&c=Products%3ASimaPro%3ASP_Tutorials&fs=Search&pn=1`.

[156] thinkstep, "What is GaBi Software n.d.." `https://www.gabi-software.com/america/overview/what-is-gabi-software/`.

[157] V. Stanciulescu and J. S. Fleming, "Life cycle assessment of transportation fuels and ghgenius," in *2006 IEEE EIC Climate Change Conference*, pp. 1–11, IEEE, 2006.

[158] Squared Consultants Inc., "GHGenius n.d.." `https://www.ghgenius.ca/index.php`.

[159] M. Q. Wang, "Greet 1.5-transportation fuel-cycle model-vol. 1: methodology, development, use, and results.," tech. rep., Argonne National Lab., IL (US), 1999.

[160] E. Kasseris, N. S. Goteti, S. Kumari, B. Clinton, S. Engelkemier, S. Torkamani, T. Akau, and E. Gençer, "Highlighting and overcoming data barriers: creating open data for retro-

spective analysis of US electric power systems by consolidating publicly available sources," *Environmental Research Communications*, vol. 2, p. 115001, nov 2020.

[161] I. Miller, M. Arbabzadeh, and E. Gençer, "Hourly power grid variations, electric vehicle charging patterns, and operating emissions," *Environmental Science Technology*, 2020.

[162] M. J. P. on the Science and P. of Global Change, "Economic projection & policy analysis model," 2020.

[163] J. Wu and S. Azarm, "Metrics for quality assessment of a multiobjective design optimization solution set," *Journal of Mechanical Design*, vol. 123, no. 1, p. 18–25, 2001.

[164] M. I. G. Salema, A. P. Barbosa-Povoa, and A. Q. Novais, "An optimization model for the design of a capacitated multi-product reverse logistics network with uncertainty," *European Journal of Operational Research*, vol. 179, no. 3, p. 1063–1077, 2007.

[165] C. D'Ambrosio, A. Lodi, S. Wiese, and C. Bragalli, "Mathematical programming techniques in water network optimization," *European Journal of Operational Research*, vol. 243, no. 3, p. 774–788, 2015.

[166] S. Twaha and M. A. Ramli, "A review of optimization approaches for hybrid distributed energy generation systems: Off-grid and grid-connected systems," *Sustainable Cities and Society*, vol. 41, p. 320–331, 2018.

[167] A. Y. Saber and G. K. Venayagamoorthy, "Intelligent unit commitment with vehicle-to-grid —a cost-emission optimization," *Journal of Power Sources*, vol. 195, no. 3, p. 898–911, 2010.

[168] J. Gong and F. You, "Sustainable design and synthesis of energy systems," *Current Opinion in Chemical Engineering*, vol. 10, p. 77–86, 2015.

[169] C. Cui, X. Li, H. Sui, and J. Sun, "Optimization of coal-based methanol distillation scheme using process superstructure method to maximize energy efficiency," *Energy*, vol. 119, p. 110–120, 2017.

[170] M. Kermani, A. S. Wallerand, I. D. Kantor, and F. Maréchal, "Generic superstructure synthesis of organic rankine cycles for waste heat recovery in industrial processes," *Applied Energy*, vol. 212, p. 1203–1225, 2018.

[171] A. Mitsos, N. Asprion, C. A. Floudas, M. Bortz, M. Baldea, D. Bonvin, A. Caspari, and P. Schäfer, "Challenges in process optimization for new feedstocks and energy sources," *Computers Chemical Engineering*, vol. 113, p. 209–221, 2018.

[172] Y. Li and R. Zhang, "Study on the operation strategy for integrated energy system with multiple complementary energy based on developed superstructure model," *International Journal of Energy Research*, 2019.

[173] B. Müller, R. Kuhlmann, and S. Vigerske, "On the performance of nlp solvers within global minlp solvers," in *Operations Research Proceedings 2017* (N. Kliewer, J. F. Ehmke, and R. Borndörfer, eds.), (Cham), pp. 633–639, Springer International Publishing, 2018.

[174] D. Kourounis, A. Fuchs, and O. Schenk, "Toward the next generation of multiperiod optimal power flow solvers," *IEEE Transactions on Power Systems*, vol. 33, no. 4, pp. 4005–4014, 2018.

[175] L. Moretti, G. Manzolini, and E. Martelli, "Milp and minlp models for the optimal scheduling of multi-energy systems accounting for delivery temperature of units, topology and non-isothermal mixing," *Applied Thermal Engineering*, vol. 184, p. 116161, 2021.

[176] X. Zheng, G. Wu, Y. Qiu, X. Zhan, N. Shah, N. Li, and Y. Zhao, "A minlp multi-objective optimization model for operational planning of a case study cchp system in urban china," *Applied Energy*, vol. 210, p. 1126–1140, 2018.

[177] A. Barbosa-Póvoa and C. Pantelides, "Design of multipurpose plants using the resource-task network unified framework," *Computers Chemical Engineering*, vol. 21, p. S703–S708, 1997.

[178] Y. Nie, L. T. Biegler, J. M. Wassick, and C. M. Villa, "Extended discrete-time resource task network formulation for the reactive scheduling of a mixed batch/continuous process," *Industrial Engineering Chemistry Research*, vol. 53, no. 44, p. 17112–17123, 2014.

[179] P. M. Castro, L. Sun, and I. Harjunkoski, "Resource–task network formulations for industrial demand side management of a steel plant," *Industrial Engineering Chemistry Research*, vol. 52, no. 36, p. 13046–13058, 2013.

[180] P. Liu, E. N. Pistikopoulos, and Z. Li, "Decomposition based stochastic programming approach for polygeneration energy systems design under uncertainty," *Industrial Engineering Chemistry Research*, vol. 49, no. 7, p. 3295–3305, 2010.

[181] A. Pertsinidis, I. Grossmann, and G. Mcrae, "Parametric optimization of milp programs and a framework for the parametric optimization of minlps," *Computers Chemical Engineering*, vol. 22, p. S205–S212, 1998.

[182] A. Bischi, L. Taccari, E. Martelli, E. Amaldi, G. Manzolini, P. Silva, S. Campanari, and E. Macchi, "A detailed milp optimization model for combined cooling, heat and power system operation planning," *Energy*, vol. 74, p. 12–26, 2014.

[183] Z. Li, D. Gao, L. Chang, P. Liu, and E. Pistikopoulos, "Hydrogen infrastructure design and optimization: A case study of china," *International Journal of Hydrogen Energy*, vol. 33, no. 20, p. 5275–5286, 2008.

[184] M. Mikolajková, H. Saxén, and F. Pettersson, "Linearization of an minlp model and its application to gas distribution optimization," *Energy*, vol. 146, p. 156–168, 2018.

[185] B. Bahl, J. Lützow, D. Shu, D. E. Hollermann, M. Lampe, M. Hennen, and A. Bardow, "Rigorous synthesis of energy systems by decomposition via time-series aggregation," *Computers Chemical Engineering*, vol. 112, p. 70–81, 2018.

[186] M. Haller, S. Ludig, and N. Bauer, "Decarbonization scenarios for the eu and mena power system: Considering spatial distribution and short term dynamics of renewable generation," *Energy Policy*, vol. 47, p. 282–290, 2012.

[187] L. Kotzur, P. Markewitz, M. Robinius, and D. Stolten, “Time series aggregation for energy system design: Modeling seasonal storage,” *Applied Energy*, vol. 213, p. 123–135, 2018.

[188] J. A. Elia and C. A. Floudas, “Energy supply chain optimization of hybrid feedstock processes: A review,” *Annual Review of Chemical and Biomolecular Engineering*, vol. 5, no. 1, p. 147–179, 2014.

[189] C. D. Demirhan, W. W. Tso, J. B. Powell, and E. N. Pistikopoulos, “A multi-scale energy systems engineering approach towards integrated multi-product network optimization,” *Applied Energy*, vol. 281, p. 116020, 2021.

APPENDIX A

BACKGROUND INFORMATION

A.1 Introduction

Ensuring access to reliable, affordable, and clean energy to a growing world population, with a growing energy demand, while simultaneously limiting the rise in global temperatures to under 2^0C compared to pre-industrial levels over the next three decades is amongst the defining challenges of the 21^{st} century [67, 68, 69]. While achieving net-carbon neutrality in itself remains a significant challenge, it is also imperative to account for historic emissions. This would require thorough analyses of contemporary energy systems to identify transition pathways that effectively decarbonize multiple facets of human consumption such as the generation and deployment of energy, and the production and transport of manufactured goods.

Declining trends in the cost of renewable energy technologies raise the prospect of a cost-competitive transition towards a carbon-neutral energy system [70]. A transition of this scale will cause a large-scale shift in primary energy supply, which is likely to also transform downstream stages of energy conversion. Notably, technologies for energy generation, energy distribution to residential as well as commercial establishments, production of synthetic fuels and chemicals, and electrified transportation will need to be evaluated and considered as a part of a large, dynamic, and integrated system.

Electrification has the potential to enable decarbonization across all the aforementioned sectors, albeit with varying degrees of penetration. A low-carbon energy landscape will potentially involve integrated value chains of multiple energy sectors to exploit interconnections and synergies [71]. Additionally, the transition will require the identification of solutions that can address decarbonization of end-uses where electricity use is currently challenged. In this context, hydrogen is an appealing energy carrier but another promising prospect is the utilization of hydrogen to sustainably produce chemicals that can be easily stored and transported and hence can serve as alternative energy carriers *energy carriers*. We discuss hydrogen, ammonia, and methanol for this utility in sub-section A.2.3.

The trend in adoption of renewable energy technologies is encouraging; renewables constituted roughly one-third of the overall global energy capacity in 2018, with the biggest portion of the recent capacity expansion coming from variable renewable energy(VRE) sources like solar and wind technologies [72]. Solar irradiance and wind speeds are subject to intermittency, seasonal variability, and uneven geographical distribution, which often result in low capacity utilization and prohibitive costs in the absence of energy storage technologies [73, 74]. Such technical constraints can limit the role for VRE resources in the low-carbon energy transition if appropriate mitigation strategies are not pursued [75, 76]. Also, considering the lifetime of the existing conventional energy generation systems and the need for further cost reductions in renewable energy generation and storage technologies, many projections support the claim that this energy transition will take decades [14, 77, 13, 78]. Subsequently, the transition will comprise multi-step pathways with hybrid portfolios of primary energy sources, including renewables, fossil fuels, and nuclear energy, that vary with local resource availability and demands [79].

Moreover, while decarbonization is the ultimate goal, the shift towards a low-carbon system should also be consistent with the United Nations'(UN) sustainable development goals(SDGs), such as goal 6 which aims to realize access to clean water, goal 12 which promotes responsible consumption, and other ancillary goals like 14 and 15 which seek to reduce environmental impact and promote economic equity [80]. Noticeably, given that energy supply chains span multiple regions or even continents, it has become imperative to consider the life-cycle impact of existing and emerging processes, products, and technologies - some examples includes battery storage, plastics, as also the manufacturing of durable goods like consumer electronics and automobiles [81]. Furthermore, the interlinkages between supply chains of multiple products and services, and the geographical distribution of their impact need to be evaluated [82]. Technical and operational advances in recycling, reprocessing, and reuse all contribute to a sustainable and circular economy by improving material utilization and processing capabilities.

Disruptions such as extreme weather and socio-economics events also highlight how the increased interdependence between various energy infrastructures could pose reliability challenges. Diversified feedstocks and integrated generation technologies with due consideration given to reliability and flexibility can improve system resiliency. Weather related disruptions such as floods and droughts, pest attacks, and equipment failures have been considered while optimizing biomass supply chains [83]. Approaches have also focused on identifying optimal storage locations and harvesting schedules in the context of weather related phenomena and moisture content of biomass [84]. Some counter measures taken in times of disruptions tend to gain acceptance, and may even serve as harbingers of larger shifts in the public mindset. For example, the trade-offs of flexible working or 'work from home' have been studied in the past [85]. However, the restrictions placed in response to COVID-19 necessitated a flexible attitude towards work. Claims about increase in worker productivity and economic benefits, if substantiated, could lead to wider acceptance. Time and energy saved due to the reduced need for transportation could further motivate this change. Moreover, reliability and resilience in energy systems needs to be carefully evaluated. Unprecedented situations, like the ongoing COVID-19 pandemic, also provide quantifiable insights into how energy demand and utilization, air quality and pollution are affected in times of disruptions [86, 87]

It is imperative to consider the variabilities, interconnections and trade-offs between the available transition pathways. Given the scale and integrated nature of energy systems, decision-support tools to study them and the underlying technological and policy implications for the energy transition also tend to be large in scope. these models tend to be large and some of the sub-processes can be non-linear. To address this complexity and to make the models computationally tractable, various holistic as well as data-driven analytical methods have been developed [88, 89]. This enables the development of decision-making tools that allow us to characterize and compare the impacts of various energy transition scenarios. A multi-decade scenario is both time and location dependent by definition, and thus the decision-making tools need to account for spatial as well as temporal variability of available resources, technologies, production targets, and policy choices

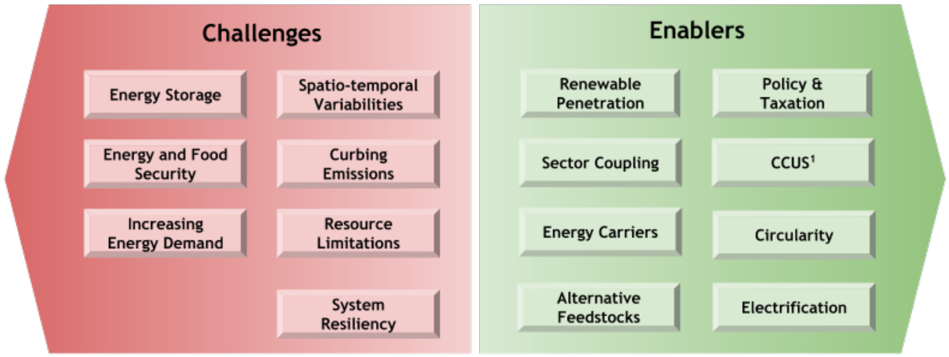

Figure A.1: Key challenges to and enablers of the energy system transition. 1 - Carbon Capture Utilization and Storage

over different geographic scales.

A.2 Key opportunities and challenges in energy transition scenario analyses

Global awareness on issues in sustainability has inspired the scientific community to identify transition scenarios that improve energy and material utilization, augment the efficiency and output of generation technologies, while also curbing emissions. These concerns were formally explicated in the Paris Agreement within the framework of the United Nations Framework Convention on Climate Change (UNFCCC) in April 2016. Almost all of the 196 member countries of the UN have committed to this effort by submitting Intended Nationally Determined Contributions (INDCs). This remains a significant step in aligning regional efforts towards mitigating global warming, reducing air pollution, and ensuring energy security. The much discussed goal to restrict global warming to below $2°C$, as compared to pre-industrialization levels, is indeed ambitious in scale, but necessary. Moreover, studies have indicated the need for an even more aggressive approach [90]. To achieve this target, it is imperative to not only completely mitigate generation but also capture and sequester carbon dioxide from the atmosphere.

Combined, the energy sector contributed to 72% of the global emission of GHGs in 2020 [91]. According to the US Energy Information Administration (EIA), 78.5% of the US primary energy consumption in June 2020 was sourced from fossil fuels such as coal, petroleum, and natural gas

[92]. Furthermore, the transportation sector is heavily dependent on petroleum products with a 95% share [92]. In the US itself, the use of fossil fuels added 1,691 million metric tons of CO_2 to the atmosphere in 2019 [92]. Meeting the target of net-zero carbon emissions by 2050 will require approaches that can substantially control emissions, improve resource utilization, and reduce the cost of energy generation. Along with nuclear, geothermal, hydro, biomass and energy carriers such as hydrogen, ammonia and methanol, solar and wind present a promising opportunity in reducing our dependence on fossil fuels.

Although the relative abundance of renewable resources and a marked decline in the cost of renewable generation technology have driven much of the adoption of renewables, policy can proselytize these efforts by encouraging consumers to explore sustainable options. However, inferring from historical trends on how the shares of primary sources in the mix have evolved, it appears that fossil fuels will likely remain relevant for at least a few more decades. Natural gas, a cleaner and more energy-dense fossil fuel, has become the preferred energy source in the industrial, commercial, and residential sector, especially in regions like US where its supply is abundant through domestic production. Similarly, direct electricity has increased its share in the commercial as well as the residential sector - for example, the share of direct electricity use in US residential and commercial sectors increased from 20.69% to 21.17% and 17.40% to 18.15% respectively, over the period 2000 to 2019 [92]. Electrification is powered by a growing share of natural gas and renewables along with a significant contribution from nuclear energy, and some decreasing contribution by coal. Studies have consistently shown the life cycle emission values of GHGs, NO_x, and SO_2 for renewable energy generation technologies to be significantly lower as compared to conventional technologies [93, 94]. The contribution comes largely from direct emissions for fossil fuels, fuel sourcing for nuclear and biomass, and infrastructural projects in the case of renewables [95].

Fig A.1 provides an overview of the opportunities and challenges, and the key analytical approaches and considerations for a multiscale energy system transition over the next three decades. In the subsequent subsections, we discuss the major challenges towards the large-scale adoption of renewables, and provide an overview of technologies and methodologies needed to address them.

A.2.1 Geographic and temporal challenges in renewable integration

Research focused on developing strategies to deal with this gap in renewable generation potential and energy demand have utilized a variety of approaches. These include technical approaches such as, predictive control for optimal dispatch of electricity, and the determination of optimal design and deployment of unit processes [96, 97]. Other approaches have focused on consumer behaviour with regards to pricing and public awareness towards the environmental cost of consumption [98].

Accurate predictions of generation outputs are imperative towards robust planning and scheduling. In the case of solar, DNI is a good indicator of solar potential. However, the performances of PV systems are also affected by cloud cover, surface azimuth and tilt, albedo, and the orientation of PVs. Like solar, wind too is subject to temporal and seasonal variations, as well as localized wind flow patterns. Such variabilities ensure limited control over the power output. Intermittency is a defining challenge in the penetration of renewables. In contrast, carbon-intensive feedstocks such as coal and natural gas permit a greater degree of process control which allows energy providers to respond dynamically to temporal variations in demand.

Furthermore, seasonal and weather-related phenomena vary significantly with geography. Constraints tend to have a local resolution, with access to resources and demand profiles being defining factors. The demand for energy, in itself, is sensitive to patterns of human movement and consumption over different geographic and temporal scales. Individually, optimizing the governing power generation processes and ignoring the synergies between feedstocks, production networks and supply chains will provide sub-optimal or even infeasible results for design, control and operation parameters of underlying energy conversion, storage and transport processes. It is imperative to consider each unit process as part of a larger formulation which captures both the regional and temporal variations explicitly. In sub-section A.3.2, we describe mathematical programming based approaches to simultaneously consider the design and operation of these systems. These represent, however, one of several alternative approaches to address the design and operations of renewables-dominant energy systems.

In addition to intermittency and variability in supply, renewable energy resources are also limited by their disparate geographic availability. Regions with high renewable potential are sometimes far from locations of high demand like metropolitan areas and industrial zones. Despite the recent reduction in the cost of renewable energy technologies, socio-economic and regulatory barriers for transmission infrastructure deployment need to be addressed to realize the full potential of renewable resource sites [99].

The challenges pertaining to regional disparity can be alleviated by systematically identifying and optimizing networks to increase energy transfer between regions. This transfer could be in the form of electricity flow through grids or as energy stored in batteries, synthetic fuels, and chemical energy carriers. Australia's central and northwest regions, for example, experience high levels of irradiance throughout the year [100]. Systematic efforts are being made to utilize this potential to address the energy demands in Asian countries with low renewable energy potentials relative to their domestic energy demands [101, 102]. Such endeavours can be mutually beneficial as they generate revenue and employment while utilizing the untapped renewable energy potential to provide affordable and reliable energy to assuage the gap in energy supply-demand.

The challenge in spatial and temporal mismatch clearly highlights that energy systems in the future will likely be composed of multiple competing pathways and combinations of various technologies that rely on hybrid energy sources with flexibility or complementariness across space and time. Contextually, identifying cost-effective strategies for sustainable development while maintaining access to energy, goods and services will require informed decision-making strategies that span multiple spatio-temporal scales; micro scales involving consumers, meso scales that are limited to plant boundaries, and macroscopic scales that can span one or multiple regions.

A.2.2 Interconnections and trade-offs in energy transition scenarios

The energy sector does not exist in isolation, with its interactions with the water and food sectors being very prominent. As demands in these three interconnected sectors increase, the need of decision-making strategies for energy generating and supply systems that exploit the Food-Energy-Water Nexus (FEW-N) are becoming more apparent [103]. Researchers are now focusing on various perspectives of the FEW-N, including resource security [104, 105], policy [106], environmental sustainability [107, 108], and waste management [109], with a great focus on the interactions and trade-offs between energy and water [103, 110]. Detailed process systems models capturing the interconnections and trade-offs between FEW-N do not yet exist at a spatial and temporal resolution sufficient for important decisions [103]. While researchers have largely focused on industrial, natural, and sociopolitical processes and systems in isolation, there is an eminent need to study those systems in tandem, while at the same time considering all three nexus dimensions [111]. The interconnected nature of FEW-N systems along with the multiple stakeholders involved, and their multiple and often conflicting objectives, make modeling difficult, while the large scales generate computational difficulties.

Furthermore, the interconnections of energy generation systems with natural resource depletion, waste management and pollution have been widely explored under the concept of Circular Economy [82]. Circular Economy (CE) is an economy that is restorative and regenerative by design [112]. Energy is at the heart of CE, with an ideal Circular Economy supply chain having closed material loops (i.e. no waste is created or no material is ever lost) but open energy loops, utilizing renewable energy. While a goal of CE is the reduction of energy usage, the increased recycling, remanufacturing, and collection of materials require a lot of energy. Therefore, decision making for energy systems and processes requires the consideration of CE aspects, and an expansion of the boundaries currently under consideration. Models for CE systems can be complex as they consider multiple processes and multiple decision makers at different scales, while the boundaries of the systems under consideration are expanded to include life-cycle aspects, making both modeling and optimization very challenging.

Process Systems Engineering tools such as multi-scale modeling, multi-objective optimization, optimization under uncertainty, mixed-integer optimization, and data analytics could provide the pillars for a holistic approach to model and optimize the interconnected energy generation and supply systems, provide trade-off solutions and aid in the understanding and analysis of the connections between energy, natural resources, food and pollution.

A.2.3 Energy carriers and storage to address spatiotemporal challenges

Studies evaluating the combined potential of renewable energy in regions have quantified geographic as well seasonal disparities and variations [113, 114]. Such spatiotemporal mismatches in the availability of energy highlight the need for dynamic, affordable, and efficient technologies to store and transport energy [115]. Furthermore, storage lends operational flexibility; robust and reliable energy systems are able to better address demand and supply side fluctuations [116]. In particular, the integration of electrochemical storage such as batteries, mechanical technologies such as compressed air energy storage(CAES) and pumped storage hydroelectricity(PSH), and chemical energy carriers has attracted significant research interest [117, 118, 119, 120, 121, 122].

PSH, which currently accounts for 95% of utility scale storage in the US [123], is limited by the availability of either naturally flowing water(open loop) or a large water body(closed loop). Meanwhile, batteries have become the choice option for mobility applications such as EVs. There have been significant improvements in the performance, longevity, sustainability as well as cost metrics of batteries [124, 125, 126]. Studies focused have focused on augmenting the technical performance of Li-ion cells have variously explored battery design aspects, electrochemistry, thermodynamics, and reaction mechanisms [127, 128, 129]. Furthermore, there has been a concerted effort to . owever, considerable bottlenecks exist in the sourcing of materials such as lithium and cobalt which also put a strain on local water resources while also releasing carcinogens and contaminants [130]. Alternatives such as sodium-sulfur (NaS) batteries, a type of molten sodium cell originally developed for EV applications in the 60s, have reemerged as a candidate as sodium can be efficiently produced by electrolysis of molten *table* salt (NaCl) [131, 132].

The significant growth in EV markets foreshadows an exponential increase in the numbers of batteries, mostly lithium-ion, to be retired in the coming years RN622. Many valuable elements and materials, such as cobalt, nickel, and manganese are contained in the waste of retired EV batteries. The recycling or repurposing of these materials post their useful life is not always technically and fiscally feasible, and can even lead to more contamination [133]. These can be viewed as valuable national assets as they provide the basis for a stable battery supply chain. Secondary production relies on used batteries has a lower environmental impact as compared to primary production from mines RN630,RN632. Battery recycling pathways, like most pyrometallurgical and hydrometallurigcal processes, are energy-intensive [134]. It has become clear that solutions that focus on addressing a singular aspect such as reducing the life cycle impact by manipulating the battery chemistry, minimizing the consumption of critical and scarce materials, and safety considerations such as exposure to hazardous materials are short-sighted [135].

Chemicals energy carriers can be used alongside batteries to address some of these shortcomings while also decarbonizing the production of chemicals. Like batteries, chemical energy carriers can improve utilization as they can be deployed in periods of high demand while being produced in periods of high availability of renewable energy. Since some options for energy carriers can be stored at atmospheric conditions with negligible losses, they can be transported over long distances. 95% of global production of hydrogen production comes from efficient yet carbon-intensive processes such as natural gas steam reforming, oil reforming, and coal gasification [136]. Conversely, Polymer Electrolyte Membrane(PEM) electrolysis of water, employed in nearly 55% of the electrolyzers and 40% of the fuel cells, produces hydrogen at a high purity(upto 99.999%) with little to no emissions during operation [137, 138]. There is also a potential to integrate hydrogen production with existing processes to improve efficiency and reduce emissions [139, 140].

Despite the surge in interest, safety considerations and the technology cost associated with hydrogen still restrict wide scale adoption. On the other hand, reduced infrastructural investments owing to well established production and distribution chains as well as relative ease of storage has brought attention to hydrogen containing chemicals such as ammonia and methanol [141]. However, almost all of the hydrogen used in ammonia plants comes from captive production from fossil feedstocks which is again carbon-intensive [142]. Integrating renewable generation and sustainable hydrogen production technologies with existing chemical production processes has a remarkable potential to reduce such emissions in a cost effective manner [143, 144].

A.2.4 Policy considerations to drive the transition

Well-designed policies are essential for accelerating global decarbonization, limiting global warming and ultimately mitigating climate change, through a collective and targeted collaboration among governments and the private sector. Financial markets, economics and technical aspects of the proposed innovations play a role towards the clean energy transition; however, policymakers play a vital role in decisively and successfully lead this transition, by re-establishing the political and social agenda, educating people and advocating the beneficial impact of this transition while providing incentives for technological innovation.

Currently, the imbalance in fiscal objectives with excessive emphasis on general income, payroll and consumption taxes, and limited emphasis on the energy taxes have contributed to wealth inequality and done little for inclusive progress. Energy prices in many countries do not reflect environmental degradation [145], even though there are studies [146] demonstrating that environmental tax reforms can indeed mitigate climate change while raising well-being, promoting income equity, and enabling economies to remain resilient and productive in the face of climate change.

Consequently, smartly designed taxes on energy and fuel use can be leveraged to drive climate action, cut existing taxes, and encourage positive economic behavior. Such taxes can achieve environmental protection at the lowest overall cost to the economy, strike a promising balance between environmental costs and benefits, and promote the adoption of technologies that reduce negative consequences on health and ecosystem [147]. To this respect, quantitative analysis is required to optimally design and assess the effects of such policies on the energy sector and on the society.

Carbon taxes schemes are considered such targeted fiscal policies, since they enable consumers to self-identify the most effective ways of reducing energy consumption by utilizing better schedules while transitioning towards environmentally conscious alternatives [148]. The substantial generated revenues can be used to offset negative macroeconomic impacts and fund initiatives towards the UN's SDGs [149]. Carbon taxes can also generate substantial domestic environmental benefits and local economies stand to benefit from the decentralized nature of implementation. However, current global carbon pricing initiatives reveal a mixed picture with regards to the type and mode of implementation of carbon pricing initiatives as well as the level of pricing. Although a rising number of jurisdictions have implemented or are considering a carbon tax, or an emission trading system (ETS), as of May 2020 only 22% of global GHG emissions are covered by carbon prices. Notably, less than 5% of these initiatives are priced at levels consistent with achieving the temperature targets that have been set in the Paris Agreement [150]. Nonetheless, jurisdictions stand to benefit from strategic, long term action plans for carbon pricing as part of their climate policy as well as for international cooperation. A recent study, revealed potential savings of around $250 billion per year in 2030 for the participating nations[151], over half of the total cost of implementation of INDCs, or a reduction of an additional 50% on global GHG emissions ($\sim$ 5 GtCO2/year in 2030) at no extra cost.

A.3 Multi-scale energy transition scenario analyses

Given the extensive size and geographic spread of energy systems, the effects of policy and technological changes often take time to culminate. Nevertheless, they profoundly impact the trajectory of the energy systems over a long time period. Decisions need to coordinate an effort of global magnitude while being mindful of local concerns and ambitions. A combination of technology and policy decisions can coordinate efforts at an enterprise scale while also being attentive to region specific economic, social, and technological characteristics. This mandates a thorough understanding of the scales at which technologies operate, the interaction between these technologies, the trade-offs between different technology and feedstock options, and a recognition of the disproportionate nature of consumption and emission.

A.3.1 Integrated Assessment Models

A set of quantitative methods and assessment tools can help identify transition pathways which draw from region-specific assessments. Such tools analyze economy-wide multi-sector dynamics and life cycles, while highlighting trade-offs to provide decision-making insights to stakeholders. Integrated assessment models (IAMs) can build the foundation for determining the mitigation pathways, as they combine insights from various disciplines under a single framework. This results in a dynamic description of the coupled energy-economy-land-climate system that covers the sources of anthropogenic GHG emissions from different sectors. This highlights the interactions, synergies, and trade-offs between sectors allowing informed decision making over a system wide level [152].

In addition, Computable General Equilibrium (CGE) models offer a powerful analytic tool to analyze and tailor energy and climate policies, and technology options to alleviate burdensome economic consequences. By design, CGE models provide economic/financial life cycle assessments of production-consumption flows. These general equilibrium models simultaneously solve for all outcomes in all markets. Though CGE models are critical to test policy and technological options and scenarios, life cycle assessment (LCA) models remain an important component for the in-depth analyses of the performance and environmental expense of technological alternatives.

LCA models typically focus on representation of the physical supply chain of multiple one-product pathways. They are important tools for the assessment of material balances and environmental impacts incurred during the cycle of production-consumption-disposal. Moreover, they comprehensively address the environmental impacts of a product from cradle to grave, which includes raw material extraction, production, use, and end of life. These pathway-level studies can be conducted using software such as openLCA [153, 154], SimaPro [154, 155], GaBi [156], GHGeneius [157, 158], and GREET [159]. LCA complements system-level analysis to explore the decarbonization of the energy sector quantitatively.

SESAME is a novel, transparent, energy-system assessment tool, which enables an assessment of GHG emissions (and costs) from approximately 80% of the economy across various sectors such as power, road-transportation, industrial, and residential at both the pathway-level and system-level [2]. This makes SESAME a powerful tool for providing a multisector representation. The system-level analysis by SESAME is enabled by the embedded power systems [160] and vehicle fleet models [161] that capture market dynamics and allow users to explore the dynamics of technology adoption and usage. The tool evaluates options, impacts, and national energy choices for exploring the impacts of relevant technological, operational, temporal, and geospatial characteristics of the evolving energy system. It focuses on life cycle analysis and techno-economic analysis (TEA) with high technology resolution (linked with the existing MIT energy-economic CGE models)[162] to provide economic information and quantify life cycle GHG emissions, as well as impacts related to criteria pollutants and water. This methodology provides a sound combination of both the environmental and economic performance of a product to help with guiding technological development and managerial decisions in a more robust way. It also helps identify and optimize trade-offs between environmental and business aspects. SESAME relies on a modular structure and it simultaneously covers various sectors and their interconnections, such as the synergies between road transportation, power, industrial and residential sectors [2]. Each module represents a life cycle step: upstream, midstream, process, carbon capture utilization and storage (CCUS), gate to user, and end use. The user can conduct pathway-level LCA by creating various individual pathways. Regarding system-level LCA, the user can group as many modules and (or) sub-modules required to represent a system.

A.3.2 Optimization-based Multi-scale Energy Systems Analysis

Given the large set of interacting variables and the complexity of energy systems models, it is practically impossible to empirically test a large variety of transition scenarios. Of particular interest are the outcomes of proposed renewable and fossil fuel pathways, effects of carbon monetization policies, and assessing circularity in the system. Systematic methods for quantitative modeling and optimization are needed to inform the decision-makers on promising courses of action. These methodologies should be able to exhaustively explore transition scenarios while accounting for the temporal and regional dynamics and variability in prices, demand, supply, and weather.

Mathematical optimization-based methods that rely on rigorous algorithms and simultaneous consideration of physics, chemistry, biology, and economics in a system have been proven to be promising tools to help decision-makers generate design and operational strategies for integrated systems. Optimization approaches aim to find the best possible solution to the problem by quantifying feasible solutions and the best possible solution [163]. Optimization methods are particularly useful when tackling systems with high degrees of freedom. Since integration naturally implies an increase in the degrees of freedom, this translates into a bigger room for improvement for energy systems. Rigorous optimization methods rely on systematic solution strategies, rather than exhaustive trial & error or heuristics-based approaches. Mathematical optimization is used to optimize design and operation of energy systems such as petroleum and chemicals processing, network flow problems, dispatch, and unit commitment problems in electric grids, etc [164, 165, 166, 167]

Optimal design of energy systems is traditionally performed through superstructure optimization. A superstructure is a systematic abstraction that consists of all possible alternatives in a system design including different technology and process integration options, operating modes conditions, interacting subsystems such as heat and power generation, products blending, or scheduling [168]. A superstructure is represented via generic mathematical equations and thus an optimization formulation can be formulated with an objective like minimizing the total system cost or maximizing the profit. Fossil hydrocarbon-based energy systems are usually optimized using the superstructure approach [169, 170]. Since such systems operate at steady state, multi-scale problems such as the unit design, process flow sheet optimization (e.g. design, planning, or scheduling), or supply chain problems can be optimized separately. Optimization of design and operation of energy systems with time-varying resources is more challenging [171, 172].

Renewable resource intermittency causes some units to remain idle or function at reduced capacities for certain periods of time, hence invalidating any steady-state assumptions. Solving a design problem with the steady-state assumption and then solving the scheduling problem for that fixed design can at best result in suboptimal, if not infeasible, operation. The hourly, daily, and seasonal fluctuations in the intermittent renewable resource availability, conversion, and delivery networks need to be addressed explicitly, thus requiring simultaneous consideration of multi-scale decisions like scheduling, process design, and optimal network flow.

If we are able to establish linear input-output relations for all processes, we can formulate linear programs (LPs) which are well studied and quite flexible. However, depending on the nature of the energy systems, linear relationships can fail to be good representations. Energy systems including petroleum refining or chemicals processing involve enthalpy, vapor-liquid equilibrium (VLE) or chemical reaction equilibrium, flow sheet optimization, or unit investment decisions with concave cost functions. These aspects are essentially nonlinear relationships, that simple LP models fail to capture. As nonlinearity is introduced to the formulations, the optimization problems become nonlinear programming (NLP) problems.

Moreover, as discrete decisions such as technology options, scheduling, or investment decisions are introduced via discrete or binary (0-1) variables to the problem, a mixed-integer problems are obtained either as mixed integer linear programming (MILP) or mixed integer nonlinear programming (MINLP) problems. Solving mixed integer programming (MIP) models has historically been a challenge; however, commercial solvers have dramatically improved over the years, especially for MILP problems, due to the significant developments in solution algorithms and increases in computational power [173, 174]. Large-scale MILP problems and modestly sized MINLP problems are now routinely solved using commercial software [175, 176]. Nevertheless, customized algorithms are still necessary to solve specific instances of MIP, especially large-scale nonconvex MINLP, problems to global optimality.

Although MINLP models are quite flexible and powerful tools to model realistic energy systems, the limitations of tractability often result in large-scale optimization formulations, especially with time-varying resources to rely on model approximation techniques and favor MILP formulations over MINLP. Regardless of the choice of linear or nonlinear models, optimization-based scenario analysis strategies and tools that consider the following as inputs:

1. Time and location dependent resource availability

2. Time and location dependent resource demand

3. Input-output relationships of the energy conversion technologies

4. Capital investment costs

5. Life-Cycle Assessments of various energy generation, storage, and conversion technologies
6. Available transportation and storage infrastructure

And return an optimal solution that comprises:

1. Process and storage unit capacities
2. Time dependent production rates for each process
3. Material and energy flow rates between processes
4. Unit commitment and operating mode selections for processes
5. Inventory management for storage of resources
6. Transportation flows of products

A.3.3 Unified representation of multi-scale models

The exhaustive consideration of the variabilities in the supply, production and demand of energy technologies and feedstock sourcing requires simultaneous consideration of time and location dependant availability of resources, energy storage, production output, and transportation within a network of candidate facilities. The need for such a unified representation of energy systems has only magnified with the increased penetration of renewable energy sources. Resource-task (also referred to as resource-technology) network (RTN) is a representation framework that allows us to consider all of these aspects in tandem [177]. RTN representation is capable of modeling systems at various scales: from a chemical plant to the design supply chain at a regional level [178, 179]

RTN formulations consist of (a) material or energy resources that can be purchased, consumed, generated, sold, stored, or transported to a different location and (b) tasks/technologies/processes that can convert material or energy resources to other resources. Subsequently, the temporal space can be discretized to allow for multi-period operation while accounting for fluctuations in time-varying resource availability. Inventory constraints keep track of all the resources entering and leaving the process network in one location and connect the consecutive time periods. Moreover, multiple locations can also be considered in the same formulation. As also, the flow of resources through the inter- and intra-process networks.

Defining each individual process mathematically allows us to formulate MINLP models. Naturally, at a multi-period and multi-location resolution, such formulations involve thousands of constraints and variables, both binary and continuous. Generating the optimal solution for problems at this scale in the presence of nonlinearity represents a significant computational challenge. These MINLPs can be solved using decomposition and parameterization techniques to approximate a sub optimal solution close to the global optimal [180, 181]. Furthermore, input-output relationships can be linearly correlated to formulate a MILP model which guarantees convergence to a global optimal. [182, 183, 184]

A complete model of an energy system entails: (i) network design constraints for production storage facilities, and transportation options (ii) selection of operating modes and throughput change constraints, (iii) general resource balance constraints, (iv) specific resource balance constraints, (v) time continuity constraints, (vi) investment and operational cost functions, (vii) emission constraints and policy considerations, and (viii) the objective function.

A.3.4 Approaches to modeling processes

The subsystems that an energy system entails vary in complexity. Striking a balance between the rigor of these models and computational tractability can be a challenge. Obviously, the quality and validity of the optimal solutions depends on the quality and validity of the models it involves. While this paper does not intend to give a thorough review of all modeling approaches, we provide a brief overview of the three most widely used approaches:

1. First principles modeling
2. Data driven modeling
3. Hybrid modeling

The first principles modeling, also called the white-box modeling, approach avails of theoretic and mechanistic insights to derive the mathematical equations for mass, momentum, and energy flows that govern the energy system. A complete physical understanding of the energy system is presumed. Conversely, data driven modeling, also called black-box modeling, assumes no physical insights while constructing mathematical relationships based solely on historical data. Data-driven modeling is effective when a mechanistic understanding of the energy system is elusive or computationally prohibitive. These data-inspired surrogate models employ techniques such as regression, classification, interpolation, or artificial neural networks(ANN) [53, 54]

Incorporating concepts from both first principles and data driven approaches, hybrid models use both theory and data to build a mathematical representation of the energy system [56, 57, 58]. An extent of physical understanding is presumed in areas which lack insight, data is utilized to guide and adjust the first-principles equations. Hybrid models have become a mainstay in energy systems engineering as energy systems become more complex. Purely theoretical approaches are not sufficient, especially in applications such as renewable energy infrastructural design and refinery manufacturing operations.

A.3.5 Scenario reduction and time-series aggregation techniques

Integrated design and operation models take advantage of the increased degrees of freedom at the expense of the increased dimensionality of the problem in terms of variables and constraints. Multi-period RTN-based formulations scale linearly with the total number of periods considered. While using linear models over nonlinear models improves the overall tractability of an optimization problem; increasing the number of time periods, the technology alternatives in a facility, and the number of facilities in the entire supply chain eventually render a model intractable. Aggregation of temporal or spatial domains in fewer clusters is a commonly used strategy to reduce the size, and consequently the tractability, of the models [185, 59, 186].

Spatial complexity at large-scale models can break the overall supply chains to multiple subregions and manage the inventories at depot locations to optimize. For tackling complexity in temporal domain, time aggregation or temporal clustering is used. Aggregating the time domain aims to decrease the number of unique (or characteristic) time periods that need to be considered in the optimization formulation to capture the daily and seasonal variability of time-dependent resources and parameters (e.g. solar, wind, power load, energy price, etc.). Clustering can be based on hours, days, weeks, or months depending on the time-series data that are clustered; it can equidistant or nonequidistant; can contain time-chronology or can be artificially constructed. Some of the commonly used clustering algorithms include k-means clustering, hierarchical clustering, or different data partitioning methods.

Clustered data inevitably results in loss of information since aggregation of data ignores individual variations. Therefore, there is always a trade-off between data accuracy and computational expense [187]. In most cases, the objective of the clustering analysis is to minimize the within cluster variance during data processing with a certain tolerance. Later, the aggregated time data is used in the optimization problem to get the optimal objective. However, it is shown by some studies that the optimal time aggregation based on clustering error does not necessarily give the best approximation to the true optimal solution. Hence, the balance between the optimal amount data aggregation and optimal network design and operation is generally obtained by using iterative decomposition algorithms.

A.4 Illustrative examples on the use of computational tools for energy transition scenario analyses

A.4.1 Power grids and car fleets - a case study of the US Southeast

A major motivation for EV adoption and incentives is emissions reduction. To have climate impact, reductions require scale, and scale cannot be analyzed accurately without modeling vehicle-grid interactions. Methodologically, estimates of the emissions impacts of high EV penetration should (1) explicitly model the dependence of power demand on EV use, and (2) justify particular assumptions re: addition mix, the mix of power added to meet the EV demand. This is illustrated by a case study, which demonstrates SESAME's approach to grid-fleet interactions.

The US Southeast contains 20% of the country's people and cars. Over the next 2 decades, solar power in the Southeast will grow substantially, according to the EIA AEO reference case [1]. Figure 1 converts AEO annual projections for 2040 into plausible hourly projections for an average day, for both generation (panels A and B) and grid emissions (panels C and D). The AEO case assumes that the passenger car fleet is 7% EVs in 2040. We call this the “low-EV” case. Our “high-EV” case assumes 50% EV penetration. The hourly generation difference between the low- and high-EV cases is represented by the red in panels A and B, and depends on charging patterns. Panel A illustrates that assuming the same grid mix between low- and high-EV cases is unrealistic. For example, relative to the low-EV case, 4am power demand is 90% higher. Assuming the same grid mix from the low- to high-EV case would effectively assume that each generation source is scaled up by 90%, including nuclear and coal power. This is unrealistic because nuclear is not being built in the US, and EV-coal correlation is unsupported. More likely, EV growth and coal generation will anti-correlate, because factors that favor EVs disfavor coal growth (e.g., battery price declines and government climate policies). Many studies on car emissions and widely used fleet models assume identical power grids between scenarios with different EV penetrations, including Argonne National Lab’s VISION model [2–4]. When EV penetration difference between 2 scenarios exceeds 20%, this assumption becomes unrealistic.

In short, at high EV penetration, the question should not be avoided: where does the red generation come from? Where does the additional power to charge the additional EVs come from? Different answers give different grid emissions. Panels C and D show the impact on grid emissions of 4 values for addition mix: identical to the generation mix in the low-EV case (as VISION assumes); all gas; 50/50 gas/renewables; and all renewables. All-renewable additions reduce grid emission intensity both at day and night (green curves), relative to the low EV case (black). All-gas additions negligibly change night grid emissions, and significantly increase midday grid emissions (red). The grid emissions curves in panels C and D can be used to estimate use emissions for any power-consuming activity, including EV use. In the high-EV case, given overnight charging, the Southeast’s 30 million EVs produce 38 MMT of emissions if the addition mix matches the low-EV case (unrealistic), and only 24 MMT if the addition mix is all renewables. Addition mix

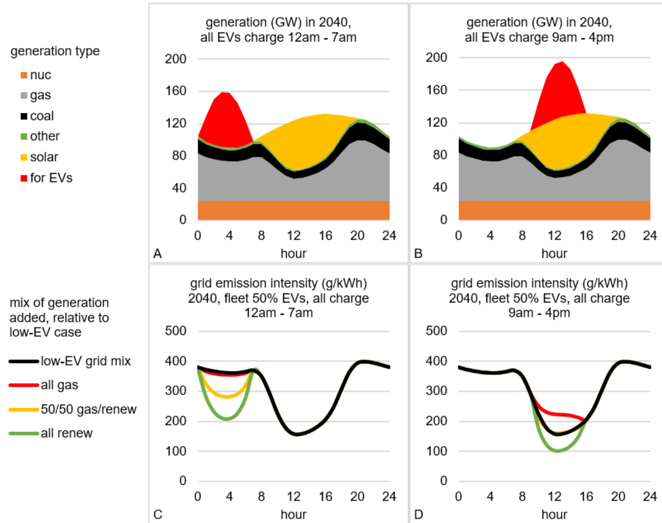

Figure A.2: (A & B) Power generation on an average day in 2040, if EV charging occurs overnight or over midday. The red generation = the generation difference between the low-EV and high-EV cases, in which EVs are 7% and 50% of passenger cars, respectively. The low-EV case is based on annual projections from the 2019 AEO [1]. Grid losses are assumed to be 4.9% [5]. (C & D) Grid emissions intensity (g/kWh) in the high-EV case, for 4 different values of "addition mix". The addition mix is the mix of generation added to meet EV power demand, relative to the low EV case. The 4 addition mixes are: identical to the grid mix in the low-EV case; all gas; 50/50 gas/renewables; and all renewables. For hours with only the black curve visible on the figure, emission intensities overlap.

matters. For context, the other 30 million passenger cars, if all ICEVs, would emit 70 MMT.

A.4.2 Multi-scale analysis of sustainable production and utilization of ammonia for energy storage and deployment

Here, to illustrate how the multi-scale energy systems engineering approach works, we can consider an ammonia production facility. Ammonia typifies the desired characteristics of an energy carrier. It can be stored as a dense liquid, either cryogenically or pressurized, and poses a relatively low flammability risk. Ammonia is consumed, through well established supply chains, as a feedstock for the production of chemicals such as fertilizers, cleaning products, and pharmaceuticals. Industrial scale production largely utilizes nitrogen separated from the air and hydrogen extracted traditionally from fossil feedstocks.

In their work, Demirhan et al. employ a process synthesis and superstructure optimization

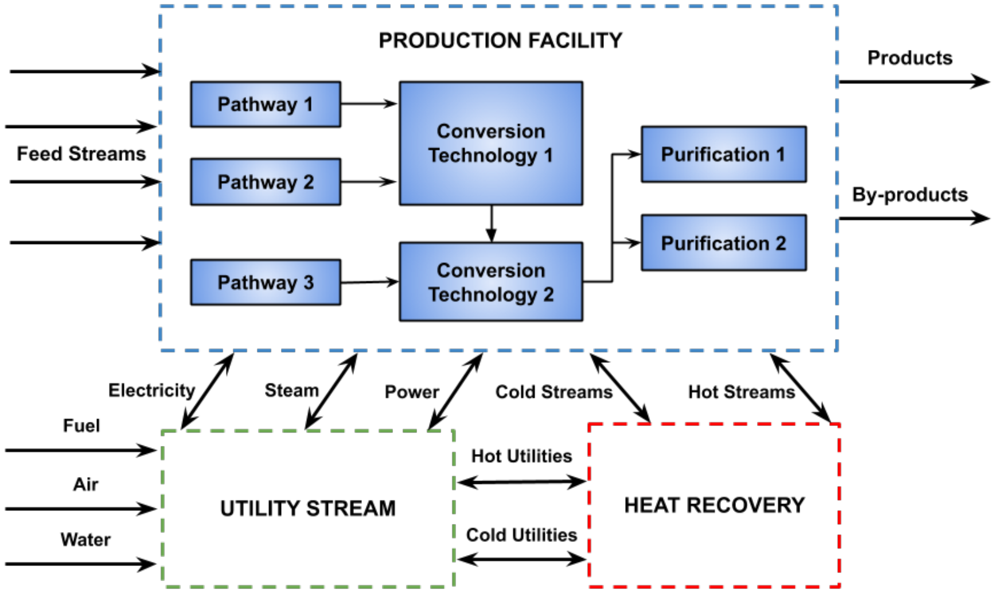

Figure A.3: Conceptual design of a process. Overall process consists of three main components: production facility, utility system, and heat recovery system

approach to compare ammonia production from natural gas, biomass, solar, and wind pathways [143]. They analyzed the economic feasibility of sustainable ammonia production by comparing the effects of GHG emission restrictions, plant location (i.e. different utility and feedstock prices and availability), and plant scales on production costs. This kind of process synthesis analysis can be applied to any energy system. The conceptual design of a generic process is illustrated in figure A.3.

It consists of three main components: (i) production facility, (ii) utility system, and (iii) heat recovery system. As illustrated in figure A.3, each production facility can consist of multiple, often competing pathways and technology alternatives. These components are highly integrated; they exchange power, heat, and process streams. The process of ammonia synthesis consists of: synthesis gas generation, water electrolysis, synthesis gas cleaning, ammonia synthesis loop, air separation, waste water treatment, heat and power integration. Each block in the conceptual design contains a multitude of submodels. Demirhan et al.'s modeling framework relies on reduced order models that were obtained via first-principle models from ASPEN PLUS or gPROMS (e.g. distillation units); enthalpy and thermodynamics data obtained from ASPEN PLUS thermophysical databases (e.g. for steam methane reforming); and black-box or hybrid models from literature for other processes (e.g. Rectisol, aMDEA for CO_2 removal). The optimization objective is to minimize the total cost of ammonia production subject to mass and energy balances, thermodynamic limitations, CAPEX and OPEX constraints, and emission restrictions. The resulting optimization problem is a nonlinear and nonconvex MINLP which contains continuous and binary decision variables. The global optimal solution was only obtained only via tailored global optimization algorithms [188]

One case study from the work focused on ammonia production in Texas, where GHG emissions were restricted to 25% of a traditional natural gas-based ammonia plant and production capacity was set as 500 metric tons/day. Investigated production routes include natural gas reforming, hardwood-type forest residue gasification, wind-powered water electrolysis, and solar-powered water-electrolysis. Results show that at the suggested emission reduction levels, biomass-based ammonia costs about \$435/ton ammonia, which is lower than natural gas-based production which costs \$472/ton. This decrease can be attributed to the costs associated with reducing the emissions in natural gas pathways and the additional revenue coming from selling electricity to the grid. Solar and wind powered electrolysis pathways are costed at \$830 and \$915/ton respectively, according to the purchase power agreement(PPA) on renewable power. Noticeably, electrolysis-based ammonia production has high production costs, due to high electricity consumption of the electrolyzers. Sensitivity studies show that water electrolysis-based ammonia production only becomes competitive when renewable electricity prices are very low. While this analysis assumed a steady supply of renewable power at a cost, the process data for ammonia production from different feedstocks were later used in the RTN formulation with variable renewable power profiles and simultaneous consideration of design and renewable power scheduling. RTN-formulation based case studies focused on low-emission, blue and green ammonia production for the purpose of hydrogen carrier and chemicals production[7, 189]

A.4.3 Infrastructure planning to drive hydrogen penetration

Hydrogen as an energy carrier has gained appeal as a driver for the decarbonization of energy, transportation, and other end-use sectors. Sustainably producing hydrogen from intermittent renewable energy resources to meet potential hydrogen demand, which vary spatially and temporally, requires significant infrastructure investments in hydrogen generation, storage and transport. To date, most studies on hydrogen infrastructure planning have focused on hydrogen use in transportation and on evaluating the trade-offs within the hydrogen supply chain, without consideration to the dynamics of its interactions with the electricity sector. The latter could include: a) hydrogen-based energy storage to manage wind, solar, and demand variability at multiple time-scales, b) flexible electrolytic hydrogen production coordinated with renewable electricity adequacy and c) transporting hydrogen or derived carriers instead of electricity to balance spatial variations in energy supply and demand. Understanding the implications of these interactions on the overall cost competitiveness of hydrogen use requires developing high-fidelity scalable decision-support frameworks with adequate representation of temporal and spatial variability in cross-sectoral interactions.

A framework has been developed by the MIT team for coordinated power and hydrogen infrastructure planning that determines the least-cost mix of electricity and hydrogen generation, storage, and transmission infrastructures to meet power and hydrogen demands subject to a variety of operational and policy constraints. The developed framework can incorporate a wide range of power and hydrogen technology options. This would include variable renewables, carbon capture and sequestration (CCUS) applied to power and hydrogen generation, transportation fuels in both gaseous and liquid forms along with a network of pipelines for hydrogen transportation. The high configurability and general applicability of the framework is enabled through strategic programming implementation. We adopt modular coding structures with various functional forms to incorporate operational constraints for each type of technology. Technology options with similar operational characteristics can be easily added to the portfolio. We also use strategic variables and set definitions in the model within and across the power and hydrogen sectors. For example, we define the power flows of technologies such as storage, generation, demand response while

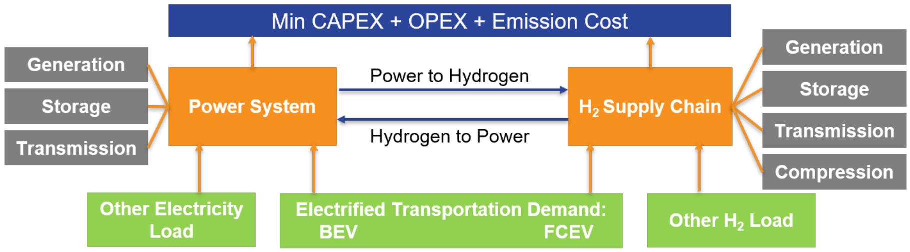

Figure A.4: Schematic of coupled power-hydrogen system model. CAPEX: capital expense. OPEX: operational expense. BEV: battery electric vehicle. FCEV: fuel cell electric vehicle.

promoting research in technologies such as electrolysis. This allows for convenient extension to couple other sectors.

The schematic of the hydrogen and power planning framework is shown in Figure A.4. The electrified transportation demand consisting of battery and fuel cell electric vehicles, are fueled by power and hydrogen systems, respectively. The model includes hourly representation of power and hydrogen system operation, that is made computationally tractable using judicious approximations and offline time-domain reduction strategies. For example, we use unsupervised learning techniques to select representative weeks of system operations to be modeled within the investment planning framework. We also use clustered linearized unit commitment for technologies with significant economies of scale and large minimum installation sizes, such as thermal power plants, natural gas hydrogen production and pipelines. Moreover, we incorporate a flexible truck scheduling and routing model, which accurately captures the travelling delay of trucks and allows for trucks to be shared across different routes and zones. We define clustered sets for full and empty trucks, which are further categorized into trucks in inventory at each zone and trucks in transit between each pair of zones.

A.4.4 Role of systematic policy frameworks in coordinating the energy transition

Quantitative analysis and meticulous planning and design is required for optimizing energy policies. To this respect, a quantitative framework, the Energy Price Index (EPIC) [66], has been developed by the Texas A&M Energy Institute team for the design, evaluation and optimization of energy policy studies. EPIC is a predictive framework that can be used as a benchmark to calculate the average price of energy to the end-use consumers in the U.S (or any other country), considering the total energy demand of the products within the energy landscape, and their corresponding prices. The non-availability of real data for the recent months as well as the forecast of future data is overcome with the introduction of a rolling horizon methodology. Having a holistic approach along with an excellent predictive ability and accuracy up to 4 years in the future, this framework can be used to evaluate, design and optimize various policy case studies retrospectively and prospectively over a range of changing parameters.

A representative policy case study [66] involves the parametric analysis of the effects of renewable energy production targets and subsidies on energy consumers. In particular, six non-fossil fuel feedstocks that are used in the electric power sector, namely, nuclear, hydroelectric power, biomass, geothermal, solar and wind, are investigated over a range of different target weights with tax credits/subsidies ranging from 0 to \$9/MMBtu for a period over the next 4 years. The results show that hydroelectric, wind, solar and geothermal power cause a drop of 0.20%, 0.14%, 0.09% and 0.02% respectively in the price of energy even with no tax credit. Conversely, nuclear and biomass require a tax credit of at least 3 \$/MMBtu and 4 \$/MMBtu respectively in order to decrease the value of energy. Potential subsidies of 9 \$/MMBtu in the nuclear, hydroelectric and wind power have the most notable effects on the price of energy, causing a drop of 2.1%, 1.67% and 1.34% respectively. Nuclear energy, due to its maximum weight of 30%, is expected to require the highest budget to provide the required subsidy.

Moreover, we can study the effects on the price of energy or, equivalently, the value of EPIC of different tax credits on wind and solar energy under distinct scenarios for their share (weight) on the electricity generation. The results are shown in Figure A.5, with the size of bubbles representing different target weights. The share of wind and solar in the electric power sector range from 5 to 13% and between 1 to 5% respectively. For low tax credit (0 or 1 \$/MMBtu), the weight of the wind energy needs to be at least 11% so as to decrease EPIC's value, whereas at the higher end of tax credits (8 or 9 \$/MMBtu), EPIC decreases even when weight contribution of wind energy

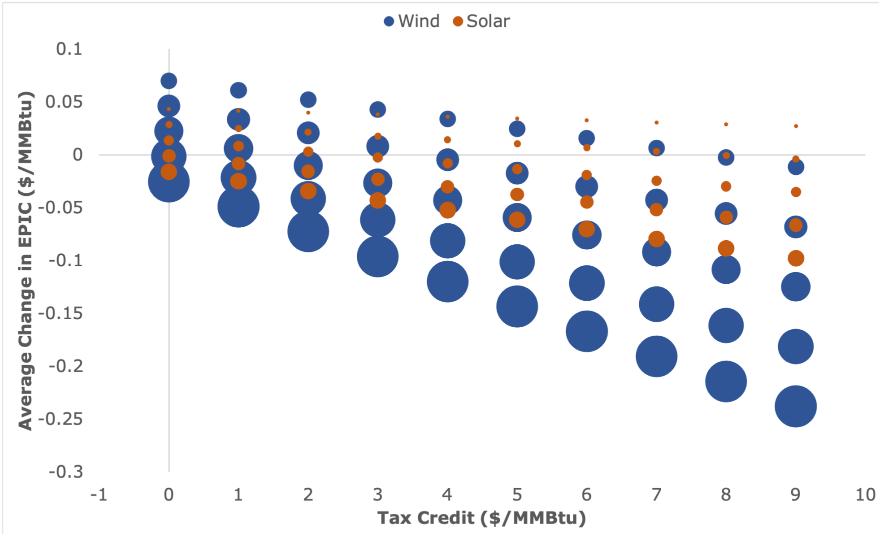

Figure A.5: Effects on the price of energy for wind and solar power at different target weights (size of the bubble) in electricity production & tax credits (2020-2024)

is minimum (5%). On the contrary, the contribution of solar energy to the electricity grid must be more than 4% and 2% for low and high tax credits respectively, in order to reduce the price of energy. Finally, as the percentage weight of wind and solar energy increases within the electric power sector, EPIC's value decreases since their levelized costs are rather low. Noticeably, when wind energy provides 13% of the electric power, EPIC drops by 0.14% even without any tax credit, whereas at the higher end of tax credit, the average drop exceeds 0.23 $/MMBtu.

APPENDIX B

MIXED INTEGER LINEAR PROGRAMMING MODEL FORMULATION

B.1 Sets

$\mathcal{I}$ processes (i)

$\mathcal{J}$ resources (j)

$\mathcal{H}$ representative seasons (h), in the base case a season is equivalent to 24h

$\mathcal{T}$ time period in hours (t)

$\mathcal{A}$ locations (a)

$\mathcal{Q}$ transportation modes (q)

$\mathcal{L}$ piece-wise linear cost segment (l)

B.2 Subsets

$\mathcal{J}_{nodischarge}$ resources (j) not to be discharged

$\mathcal{J}_{discharge}$ resources (j) to be discharged

$\mathcal{J}_{purchased}$ resources (j) to be purchased

B.3 Variables

B.3.1 Global

$Cost^{total}$ annualized total cost

GHG^{local}_{a} net GHG emission at location (a) $\forall \; a \in \mathcal{A}$

GHG^{total} total GHG emission

$Prod^{total}$ total production of hydrogen

$Inv^{excess}_{a,j,h}$ excess inventory for resource (j) in season (h) at location (a) $\forall \ a \in \mathcal{A}, j \in \mathcal{J}, h \in \mathcal{H}$

B.3.2 Non-negative

$B_{a,j,h,t}$ amount of resource (j) purchased at location (a) in time period (t) of season (h) $\forall \ a \in \mathcal{A}, j \in \mathcal{J}, h \in \mathcal{H}, t \in \mathcal{T}$

$P_{a,i,h,t}$ amount of resource consumed or produced by process (i) at location (a) in time period (t) of season (h) $\forall \ a \in \mathcal{A}, i \in \mathcal{I}, h \in \mathcal{H}, t \in \mathcal{T}$

$S_{a,j,h,t}$ amount of resource (j) sold at location (a) in time period (t) of season (h) $\forall \ a \in \mathcal{A}, j \in \mathcal{J}, h \in \mathcal{H}, t \in \mathcal{T}$

$Cap^{P}_{a,i}$ production capacity of process (i) at location (a) $\forall \ a \in \mathcal{A}, i \in \mathcal{I}$

$Cap^{S}_{a,j}$ storage capacity for resource (j) at location (a) $\forall \ a \in \mathcal{A}, j \in \mathcal{J}$

$Capex_{a,i}$ overnight capital expenditure for process (i) at location (a) $\forall \ i \in \mathcal{I}, a \in \mathcal{A}$

$Capex^{total}_{a}$ total annual capital expenditure at location (a) $\forall \ a \in \mathcal{A}$

$Inv_{a,j,h,t}$ inventory level of resource (j) sold at location (a) in time period (t) of season (h) $\forall \ a \in \mathcal{A}, j \in \mathcal{J}, h \in \mathcal{H}, t \in \mathcal{T}$

$Opex^{total}_{a}$ total annual operational expenditure at location (a) $\forall \ a \in \mathcal{A}$

$\lambda_{a,i,l}$ associated coefficient in piece-wise linear segment (l) for process (i) in at location (a) $\forall \ a \in \mathcal{A}, i \in \mathcal{I}, l \in \mathcal{L}$

B.3.3 Binary

$x^{P}_{a,i}$ equals 1 if process (i) is built at location (a) $\forall \ a \in \mathcal{A}, i \in \mathcal{I}$

$x^{S}_{a,j}$ equals 1 if storage facility for resource (j) is built at location (a) $\forall \ a \in \mathcal{A}, j \in \mathcal{J}$

$w_{a,i,l}$ equals 1 if the capacity for process (i) at location (a) is in piece-wise linear segment (l) $\forall\ a \in \mathcal{A}, i \in \mathcal{I}, l \in \mathcal{L}$

B.4 Parameters

$B^{max}_{a,j,h,t}$ maximum amount of resource (j) purchased at location (a) in time period (t) of season (h) $\forall\ a \in \mathcal{A}, j \in \mathcal{J}, h \in \mathcal{H}, t \in \mathcal{T}$

CAP^{P-max}_{i} maximum production capacity of process (i) $\forall\ i \in \mathcal{I}$

CAP^{S-max}_{j} maximum storage capacity for resource (j) $\forall\ j \in \mathcal{J}$

$CAP^{segment}_{i,l}$ capacity of process (i) at the right end of segment (l) $\forall\ i \in \mathcal{I}, l \in \mathcal{L}$

$CAPEX^{segment}_{i,l}$ capital expenditure of process (i) at the right end of segment (l) $\forall\ i \in \mathcal{I}, l \in \mathcal{L}$

$CONVERSION_{i,j}$ conversion factor of process (i) for resource (j) $\forall\ i \in \mathcal{I}, j \in \mathcal{J}$

$COST^{carbontax}$ carbon tax levied on GHG emission in \$ per tonne

$COST^{discharge}_{a,j,h,t}$ cost of discharging resource (j) at location (a) in time (h) of season (h) $\forall\ a \in \mathcal{A}, j \in \mathcal{J}, h \in \mathcal{H}, t \in \mathcal{T}$

$COST^{purchase}_{a,j,h,t}$ cost of purchasing resource (j) at location (a) in time (h) of season (h) $\forall\ a \in \mathcal{A}, j \in \mathcal{J}, h \in \mathcal{H}, t \in \mathcal{T}$

$COST^{land}_{a,i}$ land cost for process (i) at location (a) $\forall\ i \in \mathcal{I}, a \in \mathcal{A}$

$COST^{P-fix}_{i}$ fixed operating cost of process (i) $\forall\ i \in \mathcal{I}$

$COST^{P-var}_{i}$ variable operating cost of process (i) $\forall\ i \in \mathcal{I}$

$COST^{S-fix}_{j}$ fixed capital cost of storage facility for resource (j) $\forall\ j \in \mathcal{J}$

$COST^{S-var}_{j}$ variable capital cost of storage facility for resource (j) $\forall\ j \in \mathcal{J}$

$D_{a,j,h,t}$ demand for resource (j) at location (a) in time period (t) of season (h) $\forall \ a \in \mathcal{A}, j \in \mathcal{J}, h \in \mathcal{H}, t \in \mathcal{T}$

$D^{season}_{a,j,h}$ total seasonal demand for resource (j) at location (a) in season (h) $\forall \ a \in \mathcal{A}, j \in \mathcal{J}, h \in \mathcal{H}$

$D^{total}_{a,j}$ total annual demand for resource (j) $\forall \ j \in \mathcal{J}$

$UNIT_j$ parameter to convert resource (j) in kg/h to a different unit $\forall \ j \in \mathcal{J}$

$LOSS_j$ fractional loss of resource (j) in a season $\forall \ j \in \mathcal{J}$

$BigM$ a very large number

B.5 Constraints

B.5.0.1 Network design

Production capacity:

$$Cap^P_{a,i} \leq CAP^{P-max}_i.x^P_{a,i} \ \ \forall \ \ a \in \mathcal{A}, i \in \mathcal{I}$$

Storage capacity:

$$Cap^S_{a,j} \leq CAP^{S-max}_i.x^S_{a,j} \ \ \forall \ \ a \in \mathcal{A}, j \in \mathcal{J}$$

B.5.0.2 General resource balance

$$Inv_{a,j,h,t} = (1 - LOSS_j).Inv_{a,j,h,t-1} + \sum_{\forall i \in \mathcal{I}} CONVERSION_{i,j}.P_{a,i,h,t} + B_{a,j,h,t} - S_{a,i,h,t}$$

$$\forall \ \ a \in \mathcal{A}, j \in \mathcal{J}, h \in \mathcal{H}, t \in \mathcal{T}$$

B.5.0.3 Nameplate capacity constraints

$$P_{a,i,h,t} \leq Cap^{P}_{a,i} \;\; \forall \;\; a \in \mathcal{A}, i \in \mathcal{I}, h \in \mathcal{H}, t \in \mathcal{T}$$

$$Inv_{a,j,h,t} \leq Cap^{S}_{a,j} \;\; \forall \;\; a \in \mathcal{A}, j \in \mathcal{J}, h \in \mathcal{H}, t \in \mathcal{T}$$

B.5.0.4 Resource availability constraints

$$B_{a,j,h,t} \leq B^{max}_{a,j,h,t} \;\; \forall \;\; a \in \mathcal{A}, j \in \mathcal{J}, h \in \mathcal{H}, t \in \mathcal{T}$$

B.5.0.5 Demand constraints

$$\sum_{\forall t \in \mathcal{T}} S_{a,j,h,t} \leq D^{season}_{a,j,h} \;\; \forall \;\; a \in \mathcal{A}, j \in \mathcal{J}, h \in \mathcal{H}$$

$$\sum_{\forall h \in \mathcal{H}} \sum_{\forall t \in \mathcal{T}} S_{a,j,h,t} \leq \sum_{\forall t \in \mathcal{T}} D^{total}_{a,j} \;\; \forall \;\; a \in \mathcal{A}, j \in \mathcal{J}$$

B.5.0.6 No discharge constraints

$$S_{a,j,h,t} = 0 \;\; \forall \;\; a \in \mathcal{A}, j \in \mathcal{J}_{nodischarge}, h \in \mathcal{H}, t \in \mathcal{T}$$

B.5.0.7 Investment and operational cost functions

$$Cap^{P}_{a,i} = \sum_{\forall l \in \mathcal{L}} \lambda_{a,i,l}(CAP^{segment}_{i,l-1} - CAP^{segment}_{i,l}) + CAP^{segment}_{i,l}.w_{a,i,l} \;\; \forall \;\; a \in \mathcal{A}, i \in \mathcal{I}$$

$$Capex_{a,i}^{P} = \sum_{\forall l \in \mathcal{L}} \lambda_{a,i,l}(CAPEX_{i,l-1}^{segment} - CAPEX_{i,l}^{segment}) + CAPEX_{i,l}^{segment}.w_{a,i,l} \ \ \forall \ \ a \in \mathcal{A}, i \in \mathcal{I}$$

$$\lambda_{a,i,l} \leq w_{a,i,l} \ \ \forall \ \ a \in \mathcal{A}, i \in \mathcal{I}, l \in \mathcal{L}$$

$$Capex_{a}^{total} = \sum_{\forall i \in \mathcal{I}} Capex_{a,i}^{P} + \sum_{\forall j \in \mathcal{J}} (COST_{j}^{S-fix}.x_{a,j}^{S} + COST_{j}^{S-fix}.Cap_{a,j}^{S}) \ \ \forall \ \ a \in \mathcal{A}$$

$$Opex_{a}^{total} = \sum_{\forall h \in \mathcal{H}} \sum_{\forall t \in \mathcal{T}} \Big(\Big(\sum_{\forall \ i \in \mathcal{I}} (COST_{i}^{P-fix}.x_{a,i}^{P} + COST_{i}^{P-var}.P_{a,i,h,t}) \Big) \Big)$$

$$+ \sum_{\forall h \in \mathcal{H}} \sum_{\forall t \in \mathcal{T}} \Big(\Big(\sum_{\forall j \in \mathcal{J}_{purchase}} (COST_{a,j,h,t}^{purchase}.\frac{B_{a,j,h,t}}{UNIT_{j}}) + \sum_{\forall j \in \mathcal{J}_{discharge}} (COST_{a,j,h,t}^{discharge}.\frac{S_{a,j,h,t}}{UNIT_{j}}) \Big) \Big) \ \ \forall \ \ a \in \mathcal{A}$$

B.6 Objectives

$$min \ \ Cost^{total} = 0.08.Capex_{a}^{total} + Opex_{a}^{total} \ \ \forall \ \ a \in \mathcal{A}$$

$$max \ \ Prod^{total} \ \ = \sum_{\forall h \in \mathcal{H}} \sum_{\forall t \in \mathcal{T}} (S_{a,'CompressedH2',h,t} + S_{a,'LiquefiedH2',h,t}) \ \ \forall \ \ a \in \mathcal{A}$$